CAMS-TEMPO: global and European emission temporal profile maps for atmospheric chemistry modelling

Marc Guevara, Oriol Jorba, Carles Tena, Hugo Denier van Der Gon, Jeroen Kuenen, Nellie Elguindi-Solmon, Sabine Darras, Claire Granier, Carlos Pérez García-Pando

https://doi.org/10.5194/essd-2020-175
Preprint. Discussion started: 4 August 2020

Open Access Earth System Science Data Discussions

CAMS-TEMPO: global and European emission temporal profile maps for atmospheric chemistry modelling

Marc Guevara[1], Oriol Jorba[1], Carles Tena[1], Hugo Denier van der Gon[2], Jeroen Kuenen[2], Nellie Elguindi[3], Sabine Darras[3], Claire Granier[3,4], Carlos Pérez García-Pando[1,5]

[1]Earth Sciences Department, Barcelona Supercomputing Center, Barcelona, Spain
[2]TNO, Department of Climate, Air and Sustainability, Utrecht, the Netherlands
[3]Laboratoire d'Aérologie, CNRS-Université de Toulouse, Toulouse, France
[4]NOAA/Chemical Sciences Laboratory and CIRES/University of Colorado, Boulder, USA
[5]ICREA, Catalan Institution for Research and Advanced Studies, 08010 Barcelona, Spain

Correspondence to: Marc Guevara (marc.guevara@bsc.es)

Abstract. We present the Copernicus Atmosphere Monitoring Service TEMPOral profiles (CAMS-TEMPO), a dataset of global and European emission temporal profiles that provides gridded monthly, daily, weekly and hourly weight factors for atmospheric chemistry modelling. CAMS-TEMPO includes temporal profiles for the priority air pollutants (NO_x, SO_x, NMVOC, NH_3, CO, PM_{10}, $PM_{2.5}$) and the greenhouse gases (CO_2 and CH_4) for each of the following anthropogenic source categories: energy industry (power plants), residential combustion, manufacturing industry, transport (road traffic and air traffic in airports) and agricultural activities (fertilizer use and livestock). The profiles are computed on a global 0.1x0.1 deg and regional European 0.1x0.05 deg grid following the domain and sector classification descriptions of the global and regional emission inventories developed under the CAMS program. The profiles account for the variability of the main emission drivers of each sector. Statistical information linked to emission variability (e.g. electricity production, traffic counts) at national and local levels were collected and combined with existing meteorological-dependent parametrizations to account for the influences of sociodemographic factors and climatological conditions. Depending on the sector and the temporal resolution (i.e. monthly, weekly, daily, hourly) the resulting profiles are pollutant-dependent, yearly-dependent (i.e. time series from 2010 to 2017) and/or spatially-dependent (i.e. the temporal weights vary per country or region). We provide a complete description of the data and methods used to build the CAMS-TEMPO profiles and whenever possible, we evaluate the representativeness of the proxies used to compute the temporal weights against existing observational data. We find important discrepancies when comparing the obtained temporal weights with other currently used datasets. The CAMS-TEMPO data product including the global (CAMS-GLOB-TEMPOv2.1, https://doi.org/10.24380/ks45-9147, Guevara et al., 2020a) and regional European (CAMS-REG-TEMPOv2.1, https://doi.org/10.24380/1cx4-zy68, Guevara et al., 2020b) temporal profiles are distributed from the Emissions of atmospheric Compounds and Compilation of Ancillary Data (ECCAD) system (https://eccad.aeris-data.fr/). For review purposes, ECCAD has set up an anonymous repository where subsets of the CAMS-GLOB-TEMPOv2.1 and CAMS-REG-TEMPOv2.1 data can be accessed directly (https://www7.obs-mip.fr/eccad/essd-surf-emis-cams-tempo/).

https://doi.org/10.5194/essd-2020-175
Preprint. Discussion started: 4 August 2020

Open Access Earth System Science Data Discussions

1 Introduction

Spatially and temporally resolved atmospheric emission inventories are key to investigate and predict the transport and chemical transformation of pollutants, as well as to develop effective mitigation strategies (e.g. Pouliot et al., 2015; Galmarini et al., 2017). During the last decade, global and regional inventories have substantially increased spatial resolution from ~50 by 50 km (e.g. MACCity; Granier et al., 2011; EMEP-50km, Mareckova et al., 2013) to ~10 by 10 km or less (e.g. EMEP-0.1deg, Mareckova et al., 2017; TNO-MACC; Kuenen et al., 2014). Several datasets even provide emission maps for selected pollutants or study regions with resolutions as fine as 1 by 1km (e.g. ODIAC2016, Oda et al., 2018; Hestia-LA; Gurney et al., 2019; Super et al., 2020). This improvement is largely due to the emergence of new detailed, satellite-based and open-access spatial proxies such as the population maps at 1 by 1 km proposed by the Global Human Settlement Layer (GHSL) project (Florczyk et al., 2019), the global land cover maps at 300mx300m provided by the European Spatial Agency Climate Change Initiative (ESA CCI, https://www.esa-landcover-cci.org/) or the georeferenced road traffic network distributed by Open Street Maps (OSM, www.openstreetmap.org). While a clear evolution is observed in terms of spatial resolution, the improvement of the temporal representation in current state-of-the-art emission datasets has not been addressed much (Reis et al., 2011).

Using global and regional emission inventories in atmospheric chemistry models requires the original aggregated annual emissions to be broken down into fine temporal resolutions (ideally hourly) using emission temporal profiles (e.g. Borge et al., 2008; Bieser et al., 2011; Mues et al., 2014). In practice, temporal profiles are normalized weight factors for each hour of the day, day of the week and month of the year. At the global scale, the most commonly used emission temporal profiles are the monthly factors provided by the Air Pollutants and Greenhouse Gases Emission Database for Global Atmospheric Research inventory (EDGARv4.3.2; Janssens-Maenhout et al., 2019) and the Evaluating the Climate and Air Quality Impacts of Short-Lived Pollutants inventory (ECLIPSEv5.a; Klimont et al., 2017). Also at the global level, the Temporal Improvements for Modeling Emissions by Scaling (TIMES) dataset was produced to represent the weekly and hourly variability for global CO_2 emission inventories (Nassar et al., 2013). More recently, Crippa et al. (2020) developed a new set of high-resolution temporal profiles for the EDGAR inventory, which allows producing monthly and hourly emission time series and grid maps.

At European level, the temporal factors provided by the University of Stuttgart (IER) as part of the Generation of European Emission Data for Episodes (GENEMIS) project are still considered as the main reference (Ebel et al., 1997; Friedrich and Reis, 2004). The original GENEMIS profiles were later used as a basis to derive two independent datasets: (i) the EMEP temporal profiles, which provide monthly, weekly and hourly weight factors that vary per emission sector, country and pollutant (Simpson et al., 2012), and (ii) the TNO temporal profiles, which provide monthly, weekly and hourly weight factors that vary per emission sector (Denier van der Gon et al., 2011). These two sets of profiles have become over time the reference datasets under the framework of several European air quality modelling activities, including the earlier Monitoring Atmospheric Composition and Climate (MACC) project and the current Copernicus Atmosphere Monitoring Service (CAMS),

https://doi.org/10.5194/essd-2020-175
Preprint. Discussion started: 4 August 2020

among others. Other widely used regional temporal profile datasets include the North American profiles provided by the EPAs Clearinghouse for Inventories and Emissions Factors (CHIEF) (US EPA, 2019a) and the monthly profiles provided by the Multiresolution Emission Inventory for China (MEIC; Li et al., 2017).

Our goal is to provide a new set of global and European temporal profiles. Current datasets typically use the same temporal profiles for certain sectors and/or regions. For example, ECLIPSE and EMEP share the same monthly profiles for the energy sector in Europe and Russia. Similarly, TNO and EDGAR share the same monthly profiles for residential combustion and road transport (Friedrich and Reis, 2004), as well as for the energy industry (Veldt, 1992) and agriculture (Asman, 1992). In these two datasets, temporal profiles are mostly assumed to be both country- and meteorology-independent. The only exceptions are, in the case of EDGAR, for the residential and agricultural sectors, which are approximated as a function of the geographical zone: the seasonality assumed in the northern hemisphere is shifted by six months in the southern hemisphere, and a flat profile is assumed along the equator. In the case of EMEP, the reported monthly and weekly profiles do consider differences across countries but are primarily based on old sources of information from the 90s and beginning of the 00s, and subsequently neglect behavioural changes that may have happened over the last years. Moreover, variable climate conditions and changes in meteorology that may cause differences in the temporal weight factors within a country are not accounted for. In order to overcome this limitation, the ECLIPSE monthly profiles for the residential combustion sector were computed using global gridded temperature data and provided as monthly shares for each grid cell.

This work presents the Copernicus Atmosphere Monitoring Service TEMPOral profiles (CAMS-TEMPO), a new dataset of global and European emission temporal profiles for atmospheric chemistry modelling. The development of CAMPS-TEMPO comes from the need of updating the basic sources of information and improving the representation of the emission temporal variations, which was defined as a priority task within the Copernicus Global and Regional emissions service (CAMS_81) directly supporting the CAMS production chains (https://atmosphere.copernicus.eu/). Multiple socio-economic, statistical and meteorological data were collected and processed to create the profiles. The CAMS-TEMPO dataset includes monthly, weekly, daily and hourly temporal profiles for the priority air pollutants (NO_x, SO_x, NMVOC, NH_3, CO, PM_{10}, $PM_{2.5}$) and the greenhouse gases (CO_2 and CH_4) and each of the following anthropogenic source categories: energy industry, residential combustion, manufacturing industry, road transport and agriculture. Depending on the sector and temporal resolution, the profiles are either fixed (spatially-constant) or vary spatially by country or region, and can be pollutant-dependent and/or year-dependent. The CAMS-TEMPO profiles were created following the domain descriptions (resolution and geographical area covered) and emission sector classification system defined in the CAMS GLOBal ANThropogenic inventory (CAMS-GLOB_ANT) and CAMS REGional inventory for Air Pollutants and GreenHouse Gases (CAMS-REG_AP/GHG) emission inventories, also developed under CAMS_81 (Granier et al., 2019).

https://doi.org/10.5194/essd-2020-175
Preprint. Discussion started: 4 August 2020

2 Methodology

2.1 Overview

The CAMS-TEMPO dataset consists of a collection of global and regional temporal factors that follow the domain description and sector classification reported by the CAMS-GLOB_ANT and CAMS-REG_AP/GHG emission inventories. In order to better distinguish between the two sets of profiles, we refer to them as CAMS-GLOB-TEMPO (https://doi.org/10.24380/ks45-9147, global temporal profiles associated to the CAMS-GLOB_ANT inventory) and CAMS-REG-TEMPO (https://doi.org/10.24380/1cx4-zy68, regional European temporal profiles associated to the CAMS-REG_AP/GHG inventory). Depending on the pollutant source and temporal resolution (i.e. monthly, weekly, daily, hourly), the resulting profiles are reported as spatially invariant (i.e. a unique set of temporal weights for all the domain) or gridded values (i.e. temporal weights vary per grid cell). Similarly, depending on the characteristics of the input data used and approaches to compute the profiles, these can be yearly dependent and/or pollutant dependent. The spatial resolution of the gridded profiles is 0.1x0.1 deg for CAMS-GLOB-TEMPO and 0.1x0.05 deg for CAMS-REG-TEMPO. In the case of CAMS-REG-TEMPO, the domain covered by the dataset is: 30° W – 60° E and 30° N – 72°N.

Table 1 and Table 2 summarise the characteristics of each temporal profile included in CAMS-GLOB-TEMPO and CAMS-REG-TEMPO datasets, respectively. The sector classification for each case corresponds to those used in CAMS-GLOB_ANT and CAMS-REG_AP/GHG. For both temporal profile datasets, the sum of all weight factors is equal to 12 for monthly profiles, 7 for weekly profiles, 365 or 366 (in case of a leap year) for daily profiles and 24 for hourly profiles.

The following subsections describe the input data and methodologies used to compute the emission temporal profiles for each targeted sector: (i) energy industry (Sect. 2.2), (ii) residential/commercial combustion (Sect. 2.3), (iii) manufacturing industry (Sect. 2.4), (iv) road transport (Sect. 2.5), (v) aviation (Sect. 2.6) and (vi) agriculture (Sect. 2.7). The specificity of the computed profiles depends upon the degree of sectoral disaggregation used in the original CAMS inventories. For example, the CAMS-GLOB_ANT dataset reports emissions from power and heat plants and refineries under the same sector ("ene", see Table 1) and therefore a common set of temporal profiles had to be assumed for the two types of facilities. In contrast, the CAMS-REG_AP/GHG inventory reports power and heat plants under the GNFR_A category and refineries under sector GNFR_B, together with all manufacturing industries (Table 2). All the assumptions made regarding this topic are clearly stated in each subsection.

2.2 Energy industry

The temporal profiles computed for the energy industry are reported under the *ene* sector in CAMS-GLOB-TEMPO and the *GNFR_A* category in CAMS-REG-TEMPO. The temporal variability of emissions from this sector was estimated from electricity production statistics under the assumption that it largely depends upon the combustion of fossil fuels in power and

https://doi.org/10.5194/essd-2020-175
Preprint. Discussion started: 4 August 2020


Open Access Earth System Science Data Discussions

heat plants. This approximation is consistent with the definition of the *GNFR_A* sector in the CAMS-REG_AP/GHG dataset. The representativeness of the computed profiles is likely lower in CAMS-GLOB_TEMPO because the *ene* sector also includes other facilities such as refineries.

As shown in Table 1 and Table 2, the profiles reported for this sector include pollutant and country dependent monthly, weekly and hourly factors. The electricity production dataset compiled to derive profiles for this sector were as follows:

- The ENTSO-E Transparency Platform (Hirth et al., 2018; ENTSO-E, 2018): The European Network of Transmission System Operators for Electricity (ENTSO-E) centralizes the collection and publication of the electricity generation per production type for each European Member State. The information published by the Transparency Platform is collected from data providers such as Transmission System Operators (TSOs), power exchanges or other qualified third parties. The information collected included production data (MW) per country and fuel type (i.e. lignite, hard coal, natural gas, oil, biomass) at monthly (years 2010 to 2014) and hourly (years 2015 – 2017) levels.

- The US EPA emission modelling platform (US EPA, 2019a): The Environmental Protection Agency (EPA) maintains an emission modelling platform that includes, among other, processed and clean hourly emission data derived from a Continuous Emission Monitoring System (CEMS). The information collected includes hourly NO_x, SO_x and heat input data for individual power plants in years 2011 and 2014.

- The IEA electricity statistics (IEA, 2018): The International Energy Agency (IEA) provides consistent electricity statistics split by generation type (i.e. combustible fuels, nuclear, hydro, geothermal/other) and country. The information collected included monthly data for the years 2010 to 2017 for each Member country of the Organisation for Economic Co-operation and Development (OECD).

- The MBS Online (MBS, 2018): The Monthly Bulletin of Statistics (MBS) provides monthly data of the total electricity gross production per country. The information collected included data for the year 2015.

Figure 1.a illustrates the spatial coverage of the compiled dataset by source of information (i.e. ENTSO-E, US EPA, IEA and MBS). Overall, main emission producers (e.g. China, India, Europe and North America) are covered, while most of the countries with no information available are located in South America and Africa. For those countries with no data, the TNO profiles reported under the energy sector (Denier van der Gon et al., 2011) are used.

https://doi.org/10.5194/essd-2020-175
Preprint. Discussion started: 4 August 2020


Open Access Earth System Science Data Discussions

The compiled data was first analysed to assess whether interannual variability is important for this sector. Seasonal cycles were computed for different years (2010 – 2017) and countries using the IEA statistics. In the majority of the countries analysed, the monthly profiles were found to be consistent through the different years and to present small interannual variations (Fig. S1). Although some studies have pointed out a temperature dependence of the monthly electricity generation in power plants (Thiruchittampalam, 2014), we neglected it at present. Consequently, we assume the monthly temporal profiles for this sector to be the average over all the available years of data.

2.2.1 Monthly profiles

For European countries, monthly profiles were derived using the ENTSO-E dataset. The analysis of the data showed that the seasonality of electricity production varies significantly by fuel type (Fig. S1). The different use of energy sources (i.e. lignite, hard coal, natural gas, biomass and oil) implies that temporal patterns will also vary from one pollutant to the other. For each month, country and pollutant, profiles were calculated following Eq. (1):

$$M_{m,c,p} = \sum_{f=1}^{n} M_{m,c,f} \frac{FS_{c,f} * EF_{f,p}}{\sum_{f=1}^{n} FS_{c,f} * EF_{f,p}} \quad (1)$$

Where $M_{m,c,p}$ is the monthly factor for month m, country c and pollutant p; $M_{m,c,f}$ is the is the monthly factor for month m, country c and fuel f; $FS_{c,f}$ is the fuel share factor for country c and fuel f and $EF_{f,p}$ is the emission factor for fuel f and pollutant p. Fuel share factors were obtained by averaging the ENTSO-E production data for years 2010 to 2017 per country, and the emission factors were taken from the EMEP/EEA 2016 emission inventory guidebook for the priority air pollutants (EMEP/EEA, 2016; 1.A.1 Energy industries, Table 3-2, 3-3, 3-4, 3-5 and 3-7) and from the IPPC guidelines (IPCC, 2006; Volume 2: Energy, Table 2.2) for GHGs (Table 3). We note that only fuels with shares larger than 10% were considered. For instance, in the case of Austria, only hard coal (25%) and natural gas (65%) were used, and the original shares were normalised so that their sum equalled 100%. This was done to avoid introducing errors due to residual fuels, which may be related to few (or even just one) power plants.

For other countries, monthly factors by pollutant could not be developed as both the IEA and the MSB datasets do not report electricity production split by fuel type. Hence, monthly factors were derived by averaging the available production data per month and relating them to the total production in the year. For the US, NO_x and SO_x monthly profiles were derived from the corresponding hourly measured emissions reported by the EPA. The seasonality for the other pollutants (i.e. NMVOC, NH_3, CO, PM_{10}, $PM_{2.5}$, CO_2, CH_4) was linked to the measured heat input, following EPA's recommendations.

https://doi.org/10.5194/essd-2020-175
Preprint. Discussion started: 4 August 2020

2.2.2 Weekly profiles

Weekly profiles were developed for Europe and the US using the hourly electricity production data reported by ENTSO-E and US EPA, respectively. As in the case of the monthly profiles, weekly scale factors were found to significantly vary according to the type of fuel (Fig. S1). These results are in line with the conclusions of Adolph (1997), which identified three generic weekly profiles—base, medium and peak load—as a function of the type of power plant.

Pollutant-related weekly profiles were developed following the same methodology applied for obtaining the monthly weight factors (Sect. 2.2.1). For countries with no information on daily electricity production data, we used the weekly profile reported in the TNO dataset for the energy sector.

2.2.3 Hourly profiles

Hourly profiles were developed for Europe and the US using the hourly electricity production data reported by ENTSO-E and US EPA, respectively. As previously seen, large differences are observed between fuels. Profiles related to the so-called base peak load power plants (i.e. annual useful life of more than 4000 hours) present a rather flat distribution, whereas in other cases the change in energy production between day and night is relatively high (Fig. S1).

Pollutant-related hourly profiles were developed following the same methodology applied for obtaining the monthly weight factors (Sect. 2.2.1). For countries with no information on hourly electricity production data, we assumed the hourly profile reported in the TNO dataset. Some studies have suggested that the hourly variation of power plant activities may vary according to the season of the year (Thiruchittampalam, 2014). This feature is not considered in the present version of the CAMS-TEMPO profiles, and will be addressed in future releases.

2.3 Residential/commercial combustion

The temporal profiles computed for the residential/commercial sector are reported under the *res* sector in CAMS-GLOB-TEMPO and the *GNFR_C* category in CAMS-REG-TEMPO. The temporal variability of emissions for this sector is assumed to be dominated by the stationary combustion of fossil fuels in households and commercial/public service buildings. These categories are also assumed to be the main contributors to the total emissions reported by CAMS-GLOB_ANT and CAMS-REG_AP/GHG. Other combustion installations activities included under this sector (i.e. plants in agriculture/forestry/aquaculture and other stationary including military) are assumed to follow the same temporal profile.

The temporal weight factors developed for this sector include monthly, daily and hourly profiles. The monthly and daily profiles depend upon year and region, and were derived using meteorological parametrisations (Sect. 2.3.1). The hourly profiles depend upon pollutant and region (Sect. 2.3.2).

https://doi.org/10.5194/essd-2020-175
Preprint. Discussion started: 4 August 2020

Open Access Earth System Science Data Discussions

2.3.1 Monthly and daily profiles

Gridded daily temporal profiles were derived according to the heating Degree Day (HDD) concept, which is an indicator used as a proxy variable to reflect the daily energy demand for heating a building (Quayle and Diaz, 1980). This method has been proven to be successful in previous emission modelling works (e.g. Mues et al., 2014; Terrenoire et al., 2015).

The heating degree day factor ($HDD(x,d)$) for grid cell x and day d is defined relative to a threshold temperature (T_b) above which a building needs no heating (i.e. heating appliances will be switched off), following Eq. (2):

$$HDD(x,d) = \max\left(T_b - T_{2m}(x,d), 1\right) \quad (2)$$

Where $T_{2m}(x,d)$ is the daily mean 2m outdoor temperature for grid cell x and day d [ºC]. This information was obtained from the ERA5 reanalysis dataset for the period 2010 – 2017 (C3S, 2017). As shown in Eq. (2), $HDD(x,d)$ increases with the difference between the threshold and actual outdoor temperatures. A minimum value of 1 is assumed instead of 0 to avoid numerical problems when used in Eq. (3).

A challenge when using this method is to set the threshold or comfort temperature (T_b). The choice of T_b depends on local climate and building characteristics, among other. When dealing with an extended area like Europe or even the whole world, it is difficult to choose a unique T_b. This value is usually set to 18°C (e.g., Mues et al. 2014), 15.5°C (e.g. Spinoni et al. 2015) or even 15ºC (e.g. Stohl et al., 2013). Following the work by Spinoni et al. (2015), which developed gridded European degree-day climatologies, we assumed that T_b = 15.5°C, a value also suggested by the UK MET-Office. A first guess of the daily temporal factor ($FD(x,d)$) for grid cell x and day d is (Eq. 3):

$$FD(x,d) = \frac{HDD(x,d)}{\overline{HDD}(x)} \quad (3)$$

Where $\overline{HDD}(x)$ is the yearly average of the heating degree day factor per grid cell x (Eq. 4)

$$\overline{HDD}(x) = \frac{\sum_1^N HDD(x,d)}{N} \quad (4)$$

Where N = 365 or 366 days (leap or non-leap year). Considering that residential combustion processes are not only related to space heating but also to other activities that remain constant throughout the year such as water heating or cooking, a second term is introduced to Eq. 5 by means of a constant offset (f) (Eq. 5):

https://doi.org/10.5194/essd-2020-175
Preprint. Discussion started: 4 August 2020


Open Access Earth System Science Data Discussions

$$FD(x,d) = \frac{HDD(x,d)+f*\overline{HDD}(x)}{(1+f)*\overline{HDD}(x)} \quad (5)$$

Where $f = 0.2$ based on the European household energy statistics reported by Eurostat (2018) (Table 4). As observed, this share may vary depending by fuel. In the case of biofuels or coal products, which dominate the contribution to total PM emissions, space heating represents 89.1% of the residential combustion processes ($f \sim 0.1$), whereas in the case of natural gas, which is the main contributor to NO_x, the share is 77.7% ($f \sim 0.2$). Significant differences between countries are also observed for specific fuels. For instance, in Norway 100% of solid fuels are used for space heating ($f \sim 0$), whereas in Greece this share is only 65% ($f \sim 0.35$), with the remainder being attribute to water heating (27%) and cooking (8%) (Eurostat, 2018). More significant differences can be found in developing regions (e.g. Tibetan Plateau) where the share of solid biofuels used for cooking can go up to 80%. Despite these variations, a generic value of $f = 0.2$ is assumed for all regions. The investigation and proposal of different f values (as well as different T_b values) for different regions of the world will be addressed in future works.

Gridded daily temporal profiles were developed for eight years (2010 to 2017). A climatological daily profile based on the average of each day over all the available years was also produced. Monthly gridded factors were derived from the daily profiles for all the years available. We interpolated the estimated gridded daily factors from the ERA5 working domain (approx. 0.3x0.3 deg.) onto the CAMS-GLOB_ANT (0.1x0.1 deg.) and CAMS-REG_AP/GHG (0.05x0.1 deg.) grids applying a nearest neighbour approach.

2.3.2 Hourly profiles

The hourly distribution of residential/commercial combustion activities has typically been described following the profile A presented in Fig.2, used in both EMEP and TNO datasets. This hourly distribution presents one peak in the morning and another one in the afternoon, when energy consumption is supposedly higher due to increased space heating or cooking activities. We evaluated this profiles with real-world measurements of natural gas consumption for residential houses in the UK (Retrofit for the Future project, https://retrofit.innovateuk.org/), US Texas (Data Port – Pecan Street dataset, https://dataport.cloud/) and a house in Canada (Makonin et al., 2016). The measurements show the two peaks in all the profiles, although their occurrence and intensity varies due to the specific energy consumption behaviour of each house (Fig. S2). This comparison suggests that profile A is representative of emissions related to natural gas combustion.

We created a second hourly profile (Fig. 2, profile B) linked to the combustion of residential wood for space-heating purposes using as a basis information derived from citizen interviews performed in Norway and Finland (Finstad et al., 2004 and Gröndahl et al., 2010) as well as from long-term measurements of the wood burning fraction of black carbon in Athens

https://doi.org/10.5194/essd-2020-175
Preprint. Discussion started: 4 August 2020

(Athanasopoulou et al., 2017). As shown in the Fig. 2, the resulting profile B presents an intense peak during the evening hours, but not during the morning, in contrast to Profile A. It is actually a common practice in developed countries to use fireplaces and other types of wood-burning appliances mainly in the evening.

As reported by the World Health Organization (WHO), most of developing countries use wood not only for heating space purposes but also for cooking activities (Bonjour et al., 2013). We created a third profile that represents these activities (Fig. 2, profile C) based on information derived from continuous indoor $PM_{2.5}$ measurements performed in households in the eastern Tibetan Plateau (Carter et al., 2016). The profile is influenced by heating and cooking practices and therefore presents three peaks that correspond to typical morning, midday, and evening mealtimes.

The results summarised in Fig. 2 indicate that the hourly behaviour of residential combustion emissions varies according not only to the fuel type but also to the type of end-use (i.e. space heating or cooking). Both the CAMS-GLOB_ANT and CAMS-REG_AP/GHG reports total residential/commercial emission as a unique sector, without discriminating by type of fuel or end-use. Therefore, several decisions were made in order to assignm the three proposed profiles to different pollutants and regions:

- Profile A: NO_x and SO_x emissions in urban/rural areas of developed and developing countries.
- Profile B: PM_{10}, $PM_{2.5}$, CO, CO_2, NMVOC and NH_3 in urban/rural areas of developed countries.
- Profile C: All pollutants in rural areas of developing countries

The assumptions made behind this assignment are:

- Natural gas/diesel heating combustion is the main contributor to total NO_x, SO_x and CH_4 emissions
- Wood combustion is the main contributor to total PM_{10}, $PM_{2.5}$, CO, CO_2, NMVOC and NH_3 emissions
- In the urban and rural areas of developed countries wood is mainly used for heating purposes.
- In the urban areas of developing countries wood is mainly used for heating purposes.
- In the rural areas of developing countries all fuels are used both for heating and/or cooking purposes (i.e. the two activities occur at the same time).

The list of developing countries was obtained from the World Bank Country Classifications (World Bank, 2014). The discrimination of human settlements between urban and rural areas was derived from the Global Human Settlement Layer (GHSL) project (Florczyk et al., 2019; Pesaresi et al., 2019). The GHSL provides a global classification of human settlements on the base of the built-up and population density at a resolution of 1kmx1km corresponding to four epochs (2015, 2000, 1990, and 1975). The 2015 epoch was selected and the original raster was remapped onto the CAMS-GLOB_ANT (0.1x0.1 deg) and CAMS-REG_AP/GHG (0.1x0.05 deg) grids.

https://doi.org/10.5194/essd-2020-175
Preprint. Discussion started: 4 August 2020

2.4 Manufacturing industry

The temporal variability of industrial emissions is reported under the sectors *indu* (CAMS-GLOB-TEMPO) and *GNFR_B* (CAMS-REG-TEMPO). Both in the CAMS-GLOB_ANT and the CAMS-REG_AP/GHG inventories, all industrial manufacturing emissions are reported under these single categories. Hence, the same temporal pattern has to be assumed for all types of facilities (e.g. cement plants, iron and steel plants, food and beverage). For this sector, only country-dependent monthly profiles were developed due to the lack of more detailed data.

2.4.1 Monthly profiles

Country-specific monthly profiles were estimated using the Industrial Production Index (IPI), which measures the monthly evolution of the productive activity of different industrial branches, including manufacturing activities. The IPI as a monthly surrogate for industrial emissions has been used in previous studies (e.g. Pham et al., 2008; Markakis et al., 2010).

The IPI data was obtained from the MBS database (MBS, 2018) which provides monthly information per country and general industrial branch (i.e. mining, manufacturing, electricity, gas and steam and water supply) for the year 2015. The manufacturing branch, which includes several divisions such as iron and steel industries, chemical industries and food and beverage products, was used to derive country-specific monthly profiles. Figure 1b shows the spatial coverage of the compiled dataset. As in the case of the energy industry sector (Fig. 1a), the lack of information mostly affects Africa and South America. For those countries without available information, the monthly profile reported in the TNO dataset under the industry sector was used (Denier van der Gon et al., 2011). In the case of China, the monthly profile reported in the MIX inventory under the *industry* sector was used (Li et al., 2017).

The time profiles are based on IPI information from 2015 and are assumed to be representative for other years. Our assumption is supported by the low inter-annual variability observed in the IPI values collected from different national statistical offices including Italy (ISTAT, 2018), Norway (SSB, 2018), Spain (INE, 2018) and the UK (ONS, 2018) (Fig. S3). Another implicit assumption made is that the constructed monthly profiles can be equally applied to all the different industrial activities reported under the *ind* and *GNFR_B* sectors. The national IPI values collected for Italy and Spain were used to compare the seasonality of individual industrial divisions against to the general manufacturing IPI monthly profile. For both countries, and up to a certain extent, it was found that all the industrial divisions (except food/beverages and petrochemical industry) follow the seasonality of the general manufacturing profile (Fig. S4), which allow concluding that the assumption made is reasonable.

https://doi.org/10.5194/essd-2020-175
Preprint. Discussion started: 4 August 2020


Open Access Earth System Science Data Discussions

2.4.2 Weekly and hourly profiles

Due to the lack of country-specific data, the fixed weekly and hourly temporal profiles provided in the TNO dataset for industry sector is used. The weekly profile assumes a flat distribution during the working days and a slight decrease during weekends. On the other hand, the hourly profile includes an increase of the activity during the central hours of the day.

2.5 Road transport

Temporal profiles for road transport emissions are reported under the *tro* sector in CAMS-GLOB-TEMPO and the *GNR_F1* (exhaust gasoline), *GNR_F2* (exhaust diesel), *GNFR_F3* (exhaust LPG gas) and *GNFR_F4* (non-exhaust) categories in CAMS-REG-TEMPO. The fact that CAMS-REG_AP/GHG traffic-related emissions are classified into four different categories (discriminated by type of process and fuel), which allows considering specific temporal features associated to each one of them (e.g. temperature dependence of CO gasoline exhaust emissions and of NMVOC non-exhaust emissions). On the other hand, in CAMS-GLOB_ANT all traffic emissions are reported under a single sector and subsequently the approach used for the development of the temporal profiles is more simplistic.

As summarised in Table 1, the CAMS-GLOB-TEMPO monthly and weekly profiles constructed for this sector are region-dependent, whereas the hourly profiles vary per region and day of the week (i.e. weekday, Saturday and Sunday). In the case of CAMS-REG-TEMPO, the constructed profiles can vary by region, pollutant, day of the week and/or year, as a function of the source sector and temporal resolution (Table 2).

Depending on the dataset and sector category, temporal emission variability is assumed to be either exclusively driven by the traffic activity data (CAMS-GLOB-TEMP, all cases) or by a combination of traffic activity data and changes in ambient temperature (e.g. CAMS-REG-TEMP, CO and NMVOC *GNR_F1*). For the first case, temporal profiles were developed using traffic count data compiled from multiple sources of information (Sect. 2.5.1). As listed in Table 5, the information was obtained from local and national open data portals, publications or through personal communications. The spatial coverage of the compiled dataset is illustrated in Fig. 1c. For the second group of profiles, the temporal variability of traffic activity was combined with meteorological parametrisations available in the literature (Sect. 2.5.2).

Considering that for each traffic count dataset the reference years are different (Table 5), we analysed the data in view of differences in the resulting profiles as a function of the year. We took the Paris city traffic data as an example since it covers a wide range of years (2013 to 2017). For each year, monthly, weekly and hourly (i.e. Wednesday and Saturday) profiles were constructed (Fig. S5). The results suggest that temporal patterns in vehicle activity do not change much over long time scales. Consequently, and following the assumptions made for the energy and manufacturing industry sectors, we assumed that the

https://doi.org/10.5194/essd-2020-175
Preprint. Discussion started: 4 August 2020

inter-annual variability can be negligible. Hence, all profiles developed only as a function of traffic count data were constructed by averaging the values (per month, day of the week or hour of the day) over all the available years.

Some of the compiled datasets (e.g. Germany and California) report the traffic counts classified by vehicle type (i.e. light-duty vehicles, LDV and heavy-duty vehicles, HDV). The monthly, weekly and hourly profiles as a function of the vehicle type showed significant differences, especially for weekly and hourly profiles (Fig. S6). HDV traffic presents a larger decrease on the weekend than LDV. Moreover, the hourly LDV profile exhibits two distinct (morning and evening) commuter-related peaks, whereas HDV shows a single midday peak. These results highlight the importance of applying separate temporal profiles to characterize traffic and associated emissions for LDV and HDV. However, in the present work this disaggregation was not considered since both the CAMS-GLOB_ANT and CAMS-REG_AP/GHG inventories report LDV and HDV-related emissions under the same pollutant sector.

2.5.1 Meteorology-independent monthly profiles

A comparison between monthly variation in traffic patterns at urban and rural locations (i.e. urban streets and highways) was performed for selected countries/regions including California, Germany, Spain and UK. For UK and California, the original traffic statistics were already discriminated by type of location. For the German and Spanish datasets, each traffic station was classified as urban or rural considering its geographical location and the GHSL human settlement classification dataset (Sect. 2.3.2). As shown in Fig. 3, while there is little seasonal variation in German urban locations, rural areas tend to exhibit a stronger seasonality, with a peak occurring during summertime, presumably due to increased recreational and vacation-related driving. The results derived from California, Spain and UK are consistent with these patterns (Fig. S7).

The datasets collected from several cities (i.e. Athens, Barcelona, Berlin, Copenhagen, London, Madrid, Mexico City, Milano, Oslo and Paris) were also used to construct monthly profiles (Fig. 4). For comparison purposes, the TNO road transport profile is also included (Denier van der Gon et al., 2011). The three southern European cities (i.e. Athens, Madrid and Milano) together with Paris present a similar pattern, with a significant decrease of the activity during the month of August due to the summer holidays. Similarly, Northern European cities (i.e. Copenhagen and Oslo) also present a decrease in summer, but of a lower intensity and during July. On the other hand, the seasonality observed in London, Berlin and Mexico City is rather flat and closer to the TNO profile.

Results in Fig. 3 and Fig.4 showed that: (i) monthly variations can significantly differ among countries and (ii) within a country, traffic regimes show differences according to the location (urban, rural). Considering all of the above, country and region (urban, rural) specific monthly profiles were constructed based on the traffic information compiled. For countries without any available temporal factors, assumptions were made considering geographical proximity. For instance, the urban profile for Scandinavian countries without data (i.e. Finland, Sweden and Iceland) was constructed by averaging the profiles of Oslo and

https://doi.org/10.5194/essd-2020-175
Preprint. Discussion started: 4 August 2020


Open Access Earth System Science Data Discussions

Copenhagen. On the other hand, the rural profile constructed for Spain was assigned to other Southern European countries (i.e. Italy, Greece, Malta, Croatia, Bosnia and Herzegovina, Montenegro, Albania, Slovenia, Cyprus and Portugal). Similarly, the seasonality in Canada was assumed to be equal to the one observed in the US. For all the countries not listed in the table, the urban/rural profiles developed for Germany were assumed. This approach may be further improved as more traffic count data becomes available. In the case of China and India, profiles were derived from the MIX emission inventory (Li et al., 2017).

Two main assumptions underlie these profiles. First, the differences among cities within a country are assumed to be small and therefore we use a unique urban profile therein. The second hypothesis was to assume that all the streets/highways located in urban/rural areas present the same seasonality. While this is a reasonable assumption overall, individual traffic count stations can show particular features. For instance, on certain highways near city entrances or crossing urban areas, traffic intensity shows a flat distribution without the typical summer anomalies. This level of detail, which would require a specific temporal profile per road segment, is out of the scope of this dataset but may be explored in future works.

2.5.2 Meteorology-dependent monthly profiles

The seasonality of traffic emissions can be affected by temperature. As shown by Zheng et al. (2014), during winter months vehicles in China produce 19% more CO and 11% more NMVOC than in the summer due to the higher contribution of cold-start emissions. This study also showed that the monthly pattern of emissions differs remarkably by latitude, which is explained by the large contribution of cold-start emissions and the relationship between latitude and temperature. More recently, Keller et al. (2017) and Grange et al. (2019) identified strong temperature dependence for diesel vehicle NO_x emissions. On the basis of measurements of real-world vehicle emissions, both studies concluded that light-duty diesel NOx emissions are highly dependent on ambient temperature, with low temperatures resulting in higher NOx emissions (up to +80% for temperatures under 0ºC in EURO5 diesel cars; Keller et al., 2017). Grange et al. (2019) also highlighted the spatial heterogeneity of the so-called “diesel low temperature NOx emission penalty” throughout Europe due to the different climate conditions.

We used available parametrizations (Eq. 6 to Eq. 8) to account for the meteorological drivers of the seasonality of CO and NMVOC gasoline-related emissions (*GNFR_F1*) (US EPA, 2015) and NO_x diesel-related emissions (*GNFR_F2*) (Keller et al., 2017):

$$FM_{CO}(x,m) = \begin{cases} e^{(-0.038*(T_{2m}(x,m)-75)}, & T_{2m}(x,m) \leq 75°\text{F} \\ 1, & T_{2m}(x,m) > 75°\text{F} \end{cases} \quad (6)$$

$$FM_{NMVOC}(x,m) = \begin{cases} e^{(-0.048*(T_{2m}(x,m)-75)}, & T_{2m}(x,m) \leq 75°\text{F} \\ 1, & T_{2m}(x,m) > 75°\text{F} \end{cases} \quad (7)$$

https://doi.org/10.5194/essd-2020-175
Preprint. Discussion started: 4 August 2020

Open Access Earth System Science Data Discussions

$$FM_{NOx}(x,m) = \begin{cases} 1.64, & T_{2m}(x,m) \leq 0℃ \\ -0.034 * T_{2m}(x,m) + 1.64, & 0℃ < T_{2m}(x,m) < 18℃ \\ 1, & T_{2m}(x,m) \geq 18℃ \end{cases} \quad (8)$$

Where $FM_{CO}(x,m)$, $FM_{NMVOC}(x,m)$ and $FM_{NOx}(x,m)$ are the CO, NMVOC, and NO_x gridded monthly profiles for grid cell x and month m; and $T_{2m}(x,m)$ is the monthly mean 2m outdoor temperature for grid cell x and month m. Note that $T_{2m}(x,m)$ is expressed in ºF in Eq. 6 and Eq. 7 and in ºC in Eq. 8. This difference is due to the fact that the first two expression are derived from the North American MOtor Vehicle Emission Simulator (MOVES), while the last one is derived from the European Handbook Emission Factors for Road Transport (HBEFA) model. Monthly gridded 2m temperature was taken from ERA5 between 2010 and 2017 (CS3, 2017). The obtained monthly profiles where normalised so that their total sum equals 12

The meteorology-dependent monthly profiles were then combined with the meteorology-independent ones (Sect. 2.5.1) so that the resulting seasonality accounts for both temperature influences and traffic activity. For CO, we used a weight factor of 45% for the temperature-dependent profiles and of 55% for the traffic activity ones, following the UK National Atmospheric Emissions Inventory (NAEI), which reports road transport annual emissions and distinguishes between cold start and hot exhaust. Due to the lack of information, we assumed the same share for all countries. Likewise, for NMVOC profiles we assumed a 33% weight for the temperature-dependent temporal factors (i.e. emissions related to cold-start) and 67% for the ones derived from traffic counts (i.e. emissions related to hot exhaust). Finally, for NO_x we assumed a 50% and 50% split, since the "diesel low temperature NOx emission penalty" affects total exhaust diesel emissions (cold start and hot).

In addition to the meteorological-dependent profiles described above, we created a specific monthly profile for NMVOC evaporative emissions (*GNFR_F4*) based on recent results obtained with the High-Elective Resolution Modelling Emission System (HERMESv3) (Guevara et al., 2020c). The HERMESv3 model computes hourly gasoline evaporative emissions from standing cars (diurnal losses) using the Tier 2 approach reported in the EMEP/EEA emission inventory guidelines 2016. Summer and winter temperature-dependent emission factors are defined for each type of vehicle as a function of the 2-m outdoor temperature obtained from the ERA5 reanalysis. The HERMESv3 model was run over Spain for year 2016 at a spatial resolution of 4x4 km and a temporal resolution of 1 hour. The results aggregated by month and normalized (orange line in Fig. 4) show a strong seasonality, with emissions increasing up to 100% during summer. We used this profile as a first step that reflects the different dynamics of exhaust and evaporative emissions. Future works may consider developing region-specific profiles for NMVOC evaporative-related emissions.

https://doi.org/10.5194/essd-2020-175
Preprint. Discussion started: 4 August 2020


Open Access Earth System Science Data Discussions

2.5.3 Weekly profiles

Country- and region- (urban, rural) specific weekly profiles were constructed based on the traffic information summarised in Table 5. In contrast to urban areas, rural traffic activity is lower during weekdays and decrease relatively less during the weekend, specially on Sundays (Fig. 3 and Fig. S7). Figure 4 shows how, depending on the location, the intensity of the weekend decrease is relatively higher (e.g. Madrid) or lower (e.g. Mexico City), which is likely due to different sociodemographic patterns. We used the weekly profile provided in the TNO dataset as the urban profile for the countries where local information is not available. Similarly, we used an average profile including data from Germany, Spain and UK as the rural profile for countries without data. The resulting profiles were assigned equally to all the traffic-related categories of both CAMS-GLOB-TEMPO and CAMS-REG-TEMPO, with the exception of NMVOC gasoline evaporation (*GNFR_4*), for which a flat profile is proposed.

2.5.4 Hourly profiles

The analysis of hourly profiles constructed per day of the week for six cities (i.e. Berlin, Madrid, Milan, Oslo, Paris and Utrecht) clearly highlights the need to create hourly profiles per day type (Fig. S9). Weekdays (i.e. Monday to Friday) tend to exhibit strong similarities and reflect commuting patterns that are typically bimodal with morning and afternoon volume peaks. Saturday and Sunday generally show the traffic activity to plateau between late morning and early evening, typically due to a decrease in commuting activity. Some studies have developed distinct hourly traffic profiles for Monday to Thursday, Friday, Saturday and Sunday (e.g. McDonald et al., 2014), and others have discriminated between weekdays and weekends (e.g. Zheng et al., 2009). CAMS-TEMPO includes hourly profiles that vary among weekdays, Saturdays and Sundays, following other studies such as Menut et al. (2012).

Hourly variations during weekdays at urban and rural locations were compared for selected countries and regions (Fig. 3 and Fig. S8). Morning traffic peaks associated with commuting are found in and near cities, but not in rural areas (see California and Guangzhou in Fig. S8). Lunch time peaks tend to be higher in rural areas, mainly due to the activity of HDV (Spain and Germany). In contrast, hourly variations on Saturday and Sunday were found to be very similar in urban and rural areas for all the available datasets (not shown). Consequently, only for weekdays we differentiated the hourly profiles of urban and rural areas. Also in this case, the GHSL dataset was used to assign the respective profiles to either urban or rural grid cells.

Weekday hourly profiles constructed for different cities are shown in Fig. 4 (bottom-left). Two groups of profiles (showed in red and blue) with similar behaviours were identified. For the first group (in red), the rush hours in the morning and in the evening can be clearly identified. The occurrence of the peaks varies from one city to another due to different sociodemographic patterns. In the second group (in blue), a maximum level of activity is reached in the morning (between 07:00 and 08:00h) that largely remains for the rest of the day-time period (i.e. 07:00 to 19:00h) and through part of the night

https://doi.org/10.5194/essd-2020-175
Preprint. Discussion started: 4 August 2020

time (i.e. 19:00 to 21:00h). The hour when traffic activity reaches the maximum level also varies from one city to the other. Besides the potential effect of different social habits, the difference between the two groups of profiles could be also associated with differences in the vehicle densities. For instance, Oslo, Utrecht and Berlin (first group) have vehicle densities of 0.6, 1.1 and 1.3 veh/km^2 (in thousands), whereas in Barcelona, Madrid and Milano (second group) the densities are much higher (i.e. 5.2, 2.2 and 3.9, respectively) (AB, 2017).

Figure 4 (bottom-right) shows the constructed Saturdays hourly profiles for selected cities. As before, two groups of profiles showing similar patterns are highlighted. The profiles related to the first group (in red) tend to present larger activity levels during day time (between 09:00h and 18:00h), whereas in the second group (in blue) weight factors are higher during night time (between 21:00 and 03:00h). A similar pattern is observed with Sunday hourly profiles (not shown).

The resulting profiles were assigned equally to all the traffic-related categories with the exception of NMVOC evaporative emissions (*GNFR_4*), in which we use a specific hourly profile based on HERMESv3 (Sect. 2.5.2). The resulting profile is shown in Fig. 4 (bottom-left and bottom-right, in yellow).

For countries without any available temporal factors, assumptions were made considering geographical proximity. For instance, the urban profile for Scandinavian countries without data (i.e. Finland, Sweden and Iceland) was constructed by averaging the profiles of Oslo and Copenhagen. On the other hand, the rural profile constructed for Spain was assigned to other Southern European countries (i.e. Italy, Greece, Malta, Croatia, Bosnia and Herzegovina, Montenegro, Albania, Slovenia, Cyprus and Portugal). Similarly, the seasonality in Canada was assumed to be equal to the one observed for the US. For other countries , the urban/rural profiles developed for Germany were assumed as default. This approach may, of course, be improved but was constrained in this study by the traffic count data availability.

2.6 Aviation

The temporal profiles developed for air traffic emissions during Landing and Take-Off cycles (LTO) in airports are reported under the *GNFR_H* category in the CAMS-REG-TEMPO dataset. Country-dependent monthly temporal profiles were constructed using airport traffic data, as described below. We could not consider this sector for CAMS-GLOB-TEMPO since it is excluded in the CAMS-GLOB_ANT inventory. Aviation emissions are reported in a separate inventory called CAMS-GLOB-AIR, in which emission from LTO cycles are reported together with climbing, descent and cruise airplane operations.

2.6.1 Monthly profiles

We collected monthly airport traffic data by reporting airport for the years 2011 to 2017 from the Eurostat statistics (Eurostat, 2019). Year 2010 was excluded from the data gathering process due to the air travel disruption in North and Central Europe caused by the Eyjafjallajökull eruption. An analysis of the seasonality observed in several airports for each individual year

https://doi.org/10.5194/essd-2020-175
Preprint. Discussion started: 4 August 2020

allowed to confirm a low interannual variability (Fig. S10). Consequently, the constructed temporal profiles were based on the average data of all the available years. Country-dependent monthly profiles were derived by aggregating the respective national airports available in the Eurostat dataset.

2.6.2 Weekly and hourly profiles

We assumed flat weekly profiles for this sector as no clear patterns could be found in the available datasets. We use a fixed hourly profile based on airport traffic from the Madrid-Barajas and Barcelona-El Prat airports (AENA, personal communication). The computed fixed profile was found to be broadly consistent with the hourly variations reported by other studies (e.g. Unal et al., 2005; Zhou et al., 2019).

2.7 Agriculture

Global and regional temporal profiles for the agricultural emissions are reported in two separate sectors: *mma* and *agr* in CAMS-GLOB-TEMPO, and *GNFR_K* and *GNFR_L* in CAMS-REG-TEMPO. In both cases, the former category only includes emissions from livestock (enteric fermentation, manure management), whereas the latter reports emissions from several activities but mainly fertilizer applications and agricultural waste burning.

For the livestock sector (*mma* and *GNFR_K*), both in CAMS-GLOB-TEMPO and the CAMS-REG-TEMPO we assumed NH_3 and NO_x to arise from the excreta of the animals and follow a meteorology-dependent temporal profile. The rest of pollutants are considered to depend upon of the animal activity (e.g. emissions of PM arise mainly from feed, CH_4 from enteric fermentation) and therefore we assumed a flat temporal profile. In the other agricultural categories (*agr* and *GNFR_L*), NH_3 emissions are assumed to be mainly related to fertilizer application, while the other criteria pollutants (i.e. NO_x, SO_x, NMVOC, CO, PM10, PM2.5) and CO_2 are dominated by agricultural waste burning. For the particular case of CH_4, which is mostly emitted from rice fields, no particular profiles are proposed yet, this will be addressed in future works. All in all, the profiles created for agricultural emissions depend on the pollutant, year and specific sector.

2.7.1 Monthly and daily profiles for livestock emissions

For the livestock sector (*mma* and *GNFR_K*), the temporal variation of NH_3 and NO_x emissions are assumed to be depend on temperature and ventilations rates (Gyldenkærne et al., 2005; Skjøth et al., 2011) (Eq. 9):

$$FD_m(x,d) = \frac{T_m(x,d)^{0.89} * V_m(x,d)^{0.26}}{\sum_{t=1}^{365} T_m(x,d)^{0.89} * V_m(x,d)^{0.26}} \quad (9)$$

where $FD_m(x,d)$ is the daily temporal profile for manure management practice m, grid cell x and day d; $T_m(x,d)$ is the average daily temperature associated to manure management practice m, grid cell x and day d (in ºC), and $V_m(x,d)$ is the

https://doi.org/10.5194/essd-2020-175
Preprint. Discussion started: 4 August 2020

average daily ventilation rate associated to manure management practice m, grid cell x and day d (in $m \cdot s^{-1}$). The manure management practices considered include housing in open barns, housing in closed barns and storage. For each category, the values of $T_m(x,d)$ and $V_m(x,d)$ are estimated following the expressions reported by Gyldenkærne et al. (2005) and Skjøth et al. (2011). For instance, in the case of storage, $V_m(x,d)$ and $T_m(x,d)$ are assumed to be equal to the 10m outdoor wind speed and 2m outdoor temperature, respectively. The meteorological information needed to compute $V_m(x,d)$ and $T_m(x,d)$ values was obtained from ERA5 for the period 2010 – 2017 (CS3, 2017).

Since both the CAMS-GLOB_ANT and CAMS-REG_AP/GHG inventories report livestock emissions under a unique category, with no discrimination by manure management practice, the computed $FD_m(x,d)$ values had to be averaged in order to derive general daily factor values ($FD(x,d)$). The averaging was performed considering country- and grid-dependent weight factors following Eq. 10:

$$FD(x,d) = \sum_{m=1}^{3} FD_m(x,d) * f(x)_m \quad (10)$$

The weight factors ($f(x)_m$) were constructed using as a basis: (i) the national EMEP emissions reported by the Centre on Emission Inventories and Projections (EMEP/CEIP, 2019) for countries that are Members of the EMEP programme and (ii) the global bottom-up inventory of NH_3 emissions (MASAGE_NH3) (Paulot et al., 2014) for the rest of the world. Table S1 summarises the weight factors used for each country. For countries not included in the list, an average weight factor is used.

The resulting gridded daily temporal profiles were developed for eight years (2010 to 2017). Using these time series as a basis, and following with the procedure described in Sect. 2.3.1, a climatological daily profile and monthly gridded factors were also produced.

2.7.2 Monthly and daily profiles for fertilizer-related emissions

The seasonality of NH_3 emissions from fertilizer application depends mainly on the magnitude and timing of fertilizer application over different crop categories (i.e. planting schedule for each crop). The proposed gridded monthly profiles for this pollutant sector are based on a mosaic of multiple bottom-up agricultural emission inventories, which include information on local crop calendars in their emission estimations. The datasets included in the mosaic are: (i) the global bottom-up gridded MASAGE_NH3 inventory (Paulot et al., 2014), (ii) the regional gridded Chinese emission inventory reported by Zhang et al. (2018), (iii) the regional gridded North American National Emission Inventory (NEI) reported by US EPA (2019b) and (iv) the regional European emission inventories reported for Denmark, Germany (Skjoth et al., 2011), (v) Poland (Werner et al., 2015) and (vi) Netherlands, France and Belgium (Backes et al., 2016).

https://doi.org/10.5194/essd-2020-175
Preprint. Discussion started: 4 August 2020

With the objective of computing daily variations, the gridded monthly profiles obtained using the aforementioned mosaic approach were combined with the daily meteorological parametrizations reported by Gyldenkærne et al. (2005) and Skjøth et al. (2011) (Eq. 11):

$$FD(x,d) = \frac{e^{0.0223 * T_{2m}(x,d)} * e^{0.0419 * W_{10m}(x,d)}}{\sum_{t=1}^{365} e^{0.0223 * T_{2m}(x,d)} * e^{0.0419 * W_{10m}(x,d)}} \quad (11)$$

where $T_{2m}(x,d)$ is the daily mean 2m outdoor temperature for grid cell x and day d [ºC]; and $W_{10m}(x,d)$ is the daily 10m wind speed for grid cell x and day d [m·s^{-1}]. Both parameters were derived from ERA5 for the period 2010 – 2017 (C3S, 2017). The resulting gridded daily temporal profiles includes eight years of data (2010 to 2017) and a climatological profile.

2.7.3 Monthly profiles for agricultural waste burning emissions

For all the other criteria pollutants (i.e. NO_x, SO_x, NMVOC, CO, PM_{10}, $PM_{2.5}$) included in the *agr* and *GNFR_L* sectors, we used the monthly gridded profiles reported by Klimont et al. (2016) for the agricultural waste burning category. This temporal representation was developed based on the timing and location of active fires on agricultural land in the Global Fire Database (GFEDv3.1) combined with annual emissions from the Greenhouse Gas and Air Pollution Interactions and Synergies (GAINS) model. The original monthly weights were remapped from the ECLIPSE source grid (0.5x0.5 deg) onto the CAMS-GLOB_ANT and CAMS-REG_AP grids applying a nearest neighbour approach.

2.7.4 Hourly profiles

The hourly distribution of agricultural emissions has typically relied on the profile reported by both TNO and EMEP datasets (Fig. 2, bottom). The profile is constructed on the idea that NH_3 emission rates from agricultural practices (fertilizer application and manure management) tend to vary with temperature, usually showing a peak in the middle of the day. Figure 2 (bottom) compares this profile with the hourly distributions derived from flux measurements performed in a fertilized corn canopy in North Carolina (Walker et al., 2013) and from direct measurements performed in a mechanically ventilated swine barn (James et al., 2012). The similarity observed between the TNO profile and the two measurement-based temporal factors is significantly high (i.e. emissions peak during the afternoon in each case, starting from 13:00 to 15:00h Local Time). We therefore maintained the TNO profile for describing the hourly variation of NH_3 agricultural emissions (both for livestock and fertilizer application).

Regarding the other criteria pollutants (i.e. NO_x, SO_x, NMVOC, CO, PM_{10}, $PM_{2.5}$) included in the *agr* and *GNFR_L* sectors, a new hourly fixed hourly temporal profile for agricultural waste burning emissions is proposed based on the work by Mu et al. (2011), where climatological mean hourly cycles were constructed using GOES WF_ABBA active fire satellite observations from full hemisphere scans during 2007–2009. The constructed profile (Fig. 2, bottom) shows a maximum peak at midday, which is consistent with high levels of midday fire emissions.

https://doi.org/10.5194/essd-2020-175
Preprint. Discussion started: 4 August 2020

3 Results and discussion

In this section, we discuss the obtained temporal profiles for CAMS-GLOB-TEMPO and CAMS-REG-TEMPO. In Sect. 3.1 the profiles are compared to independent observational datasets and in Sect. 3.2 to other existing sets of temporal profiles currently used under the framework of CAMS.

Figure 5 shows the 0.1x0.1 deg CAMS-GLOB-TEMPO gridded January and August profiles constructed for NMVOC and SO_x energy industry emissions and for manufacturing industry emissions. For the energy sector, several countries such as Spain and UK show how the seasonality significantly varies as a function of the pollutant. It is also observed that in many European countries the manufacturing industrial activity decreases during August due to summer holidays, while an increase is observed in other countries such as China.

Figure 6 shows two examples of CAMS-GLOB-TEMPO gridded daily profiles for the residential/commercial sector along with the times series at four geographically or climatically different locations (i.e. Athens; Barcelona; Buenos Aires and Oslo) for years 2010 and 2017. As expected, the largest factors occur in winter and the lowest ones in summer at all four locations. According to the results, emissions in Athens, Barcelona or Buenos Aires can be 3 to 5 times higher during the cold periods (i.e. January in Barcelona and Athens, June in Argentina) than during warm periods (August in Barcelona and Athens, January in Argentina). In Oslo both the seasonal cycle and daily variability are less pronounced than in the other locations because the differences between daily and annual mean temperatures are generally lower. There is a large inter-annual variability in the four locations. In winter of 2010, Barcelona experienced three cold outbreaks of similar intensity (in January, February and March), whereas in 2017 only one significant episode can be observed (mid-January). Similarly, in 2010 three major peaks are observed in Athens in mid-January, beginning of February and mid-December, whereas in 2017 only one episode stands out above the rest. Results clearly highlight that extreme weather events can strongly affect the temporal profiles and thereby the resulting emissions.

Figure 7 shows examples of the 0.1x0.05 deg CAMS-REG-TEMPO gridded profiles constructed for the different road transport categories, including January and August (monthly) weights for gasoline CO exhaust emissions, and both Friday and Sunday (weekly) and 09:00 and 20:00h (hourly weekday) weights for all traffic sources except NMVOC gasoline evaporation. The monthly gridded profiles clearly show the influence of outdoor temperature, with weight factors up to 2.5 times higher in January than in August in Eastern Europe and Russia. The weekly profile maps clearly show the decrease in emissions from traffic during the weekend, especially in urban areas. The hourly profiles show the high levels of traffic activity during night time in some Mediterranean countries compared of central and North European ones, and also a clear distinction between urban and rural areas.

https://doi.org/10.5194/essd-2020-175
Preprint. Discussion started: 4 August 2020

Figure 8 shows examples of CAMS-GLOB-TEMPO profiles for the different agricultural emission sources, including April and November (monthly) weights for fertilizer NH_3 emissions, daily (i.e. 2017/03/06 and 2017/07/16) weights for livestock NH_3 and NO_x emissions, and daily time series for livestock emissions over Spain and Argentina for 2010 and 2017 (Note the country daily times series are spatially aggregated as the actual patterns are variable spatially.). Concerning the fertilizer monthly factors, it is observed that the spatial resolution is not homogeneous across the domain. This is due to the different spatial resolutions of the original datasets used to construct this gridded profile: The MASAGE_NH3 emission inventory is available at a resolution of 2x2.5 degree, while the datasets used for China and USA are reported at resolutions of 0.25x0.25 deg and 12kmx12km, respectively. Despite the coarse resolution, the profiles broadly capture the different seasonality in different parts of the world, with a peak of emissions occurring in April in Europe and in November in Latin America. For the livestock sector, the largest weight factors occur during the summer and the lowest ones during the winter due to the temperature dependence. Nevertheless, and in contrast to what is observed with the residential/commercial daily factors, the signal for livestock emissions is mostly seasonal and the daily fluctuations are relatively small, which makes the interannual variability small.

3.1 Comparison to independent observational datasets

Figure 9 shows the CAMS-TEMPO monthly weight factors for SO_x energy industry in Spain and manufacturing industry in Italy compared against two independent temporal profiles based on SO_x measured emissions from all Spanish power plants (CIEMAT, personal communication) and real-world measurements of industrial natural gas consumption provided by the European Network of Transmission System Operators for Gas (ENTSOG, 2020), respectively. Correlations between the two time series are high in both cases (i.e. r= 0.84 and 0.61, respectively). In the case of energy industry in Spain both profiles show minimum levels during spring and an increase during summer due to the intensive use of air conditioning systems. In Italy, both manufacturing industry profiles present a strong decrease during August and December due to summer and Christmas holidays.

In Fig. 10 we compare our profiles for the residential sector with daily factors derived from minute-resolved measurements of natural gas from a residential house in Canada during 2013 (Makonin et al., 2016). We compared our daily factors estimated using the HDD approach for the grid cell closer to the house and considering two different values of T_b (18 and 15.5°C). In both cases, CAMS-TEMPO reproduces the temporal variation of the locally measured profile. Both at the beginning and the end of the year, the measured and HDD-based profiles show similar maximum values, which correspond to the periods when outdoor temperature reached the minimum levels (not shown). The results also show that using $T_b = 15.5$°C we obtain a slightly higher correlation than when assuming T_b = 18°C (0.81 versus 0.76).

In Fig. 11 we compare the CAMS-REG-TEMPO road transport profiles to the temporal variation of air pollutant concentrations measured in Madrid, Milano, Barcelona and and Berlin. CO and NO_2 hourly concentrations were obtained from the European

https://doi.org/10.5194/essd-2020-175
Preprint. Discussion started: 4 August 2020

Environmental Agency (EEA) download service of validated and official air quality data (EEA, 2019). Four urban traffic stations highly influenced by road transport emissions were considered for the analysis: Escuelas Aguirre (Madrid), Milano-Senato (Milano), Eixample (Barcelona) and B Neukölln-Karl-Marx-Str. 76 (Berlin).

The monthly variability of CO and NO_2 measured concentrations in Milano and Madrid were compared against the meteorology-dependent gridded monthly profiles created for CO GNFR_F1 (gasoline exhaust) and NO_x GNFR_F2 (diesel exhaust) at these locations. Weight factors from the closest grid cells closest to each station were selected for the comparison. As shown in Fig. 11 (top-left and top-right), the traffic decrease occurring during summertime in Milano and Madrid is also reproduced in the CO and NO_2 levels. At the same time, both the CAMS-REG-TEMPO profiles and the measurement-based profiles show a V shape, indicating higher emissions during winter due to the low temperatures. The correlation between the two times series is of r= 0.82 for Milano and of r= 0.74 for Madrid. we note that the seasonality of the CO and NO_2 measurements may be also influenced by other factors, including meteorology and the influence of other emission sources such as residential combustion, and subsequently a perfect correlation between the two datasets cannot be expected.

Similarly, the hourly profiles proposed for urban locations in Spain and Germany during weekdays and Sundays were compared to the hourly variation of NO_2 concentrations for Barcelona and Berlin (Fig. 11, bottom-left and bottom-right). In all cases the hourly evolution of NO_2 is mostly driven by variations accounted for in the CAMS-TEMPO profiles. For weekdays, the shift of the traffic morning/evening peaks observed between cities is also reproduced in NO_2 concentrations. Traffic and NO_2 levels in Berlin reach maximum levels between 07:00h and 08:00h LT, whereas in Barcelona the peak occurs between 08:00 and 09:00h LT. On the other hand, Sunday night time and morning NO_2 concentrations (between 23:00 and 08:00h LT) are relative higher in Barcelona than in Berlin (in relative terms), which is related to the more intense traffic activity registered in the streets.

3.2 Comparison to other temporal profile datasets

We compared the CAMS-TEMPO profiles against the profiles reported by other existing datasets. The comparison is focussed on the profiles that are currently being used for air quality modelling purposes under the framework of CAMS, namely: The global EDGARv4.3.2 (Janssens-Maenhout et al., 2019) monthly profiles (used in the CAMS global production) and the European EMEP (Simpson et al., 2012) and TNO (Denier van der Gon et al., 2011) profiles (used in CAMS regional production).

The comparison of monthly, weekly and hourly profiles for the energy industry sector in selected countries is shown in Fig. 12. It is worth noting that both TNO and EDGAR report the same profile for all countries. At the monthly level, significant differences are observed between CAMS-TEMPO and EDGAR in China and USA. In both cases, the summer peak observed in CAMS-TEMPO (presumably due to the intensive use of air conditioning systems) does not show up in EDGAR profile. In

https://doi.org/10.5194/essd-2020-175
Preprint. Discussion started: 4 August 2020

the case of Romania, all profiles show important decreases but at different times of the year: April in CAMS-TEMPO (presumably due to low use of heating/cooling devices), July in TNO/EDGAR and September in EMEP. In the UK, the patterns between the different datasets are more similar, all of them reproducing a V shape, except for the relatively flatter NMVOC emissions profiles in CAMS-TEMPO. Concerning the weekly and hourly profiles, important discrepancies are observed between CAMS-TEMPO and the factors proposed by TNO and EMEP for certain countries. In the CAMS-TEMPO weekly profiles for Austria the intensity of the weekend decrease is relatively higher, while the hourly profiles for Spain are flatter than the ones reported by TNO and EMEP.

The comparison of monthly weight factors for the residential/combustion sector indicates generally low discrepancies between the different datasets (Fig. 13). The largest difference is observed in Greece, where both CAMS-TEMPO and EMEP allocate most of the emissions during wintertime while TNO and EDGAR propose a smoother transition between this season of the year and spring/fall. Both EDGAR and CAMS-TEMPO datasets propose an almost flat profile for India, where residential fuel is mainly used for cooking activities, an activity that can be considered constant throughout the year. For the daily temporal disaggregation of emissions, TNO and EMEP propose a fixed weekly profile (not shown), which disregards the daily dynamics inferred by the heating degree day approach considered in CAMS-TEMPO (Fig. 6).

For road transport, the differences between CAMS-TEMPO and other datasets are quite significant. The monthly profiles reported by TNO, EMEP and EDGAR are almost flat, while the pollutant and meteorological dependent profiles developed in the present work suggest important decreases during summertime, especially for the case of CO (Fig. 14). At the weekly level, the TNO profile is in line with most of the city-level constructed profiles, although in some cases differences in the intensity of the weekend decrease are observed (Fig. 4, top-right). At the hourly level, the main discrepancies are observed when comparing TNO with the Saturday and NMVOC evaporative profiles of CAMS-TEMPO (Fig. 4, bottom right). It is worth noting that the hourly weekday profile constructed for Utrecht is almost perfectly correlated with TNO ($R^2 = 0.97$). This is explained by the fact that the TNO profile was estimated using Dutch traffic data.

Figure 15 shows a comparison of the monthly profiles for the agricultural sector. All the datasets selected for comparison, except for TNO, propose a unique profile for all the different agricultural activities (i.e. livestock, use of fertilizers, agricultural waste burning), which is equally applied to all emissions. The CAMS-TEMPO profiles constructed for NH_3 fertilizer emissions show how the peak significantly varies among countries (i.e. May in China, June in India, April in Spain). In the case of India and China, these peaks are consistent with the NH_3 satellite-derived seasonality shown by Warner et al. (2017). It is also worth noting the triple peak in Poland, which is related to the application timings of fertilizers (spring) and manure (summer and autumn) on crops (Werner et al., 2017). In contrast, the profiles reported by TNO and EMEP show a unique peak in April in all countries. In the case of NH_3 from livestock, the profiles show a weaker seasonality, but relevant discrepancies in the intensities and occurrences of the emission peaks are also observed (i.e. EDGAR-India, EMEP-Spain). In the case of PM_{10}

https://doi.org/10.5194/essd-2020-175
Preprint. Discussion started: 4 August 2020

emissions related to agricultural waste burning activities, the results suggest a good agreement between EMEP and CAMS-TEMPO, with most emissions occurring during fall, after the harvesting period. On the other hand, the profile proposed by TNO presents a double peak, a first one occurring during spring (March and April) and a second one during summer (August).

4 Data availability

Gridded maps with all the temporal factors (monthly, weekly, daily, hourly) per sector and year are available as NetCDF files for the global domain at a resolution of 0.1x0.1 deg (CAMS-GLOB-TEMPOv2.1, https://doi.org/10.24380/ks45-9147, Guevara et al., 2020a) and the European regional domain (30° W – 60° E and 30° N – 72°N) at a resolution of 0.1x0.05 (CAMS-REG-TEMPOv2.1, https://doi.org/10.24380/1cx4-zy68, Guevara et al., 2020b) and can be accessed through the Emissions of atmospheric Compounds and Compilation of Ancillary Data (ECCAD) system with a login account (https://eccad.aeris-data.fr/). For review purposes, ECCAD has set up an anonymous repository where subsets of the CAMS-GLOB-TEMPOv2.1 and CAMS-REG-TEMPOv2.1 data can be accessed directly (https://www7.obs-mip.fr/eccad/essd-surf-emis-cams-tempo/). In addition, constructed fixed temporal profiles are available per sector and substance in Appendix A of this work.

5 Conclusions

This paper presents the CAMS-TEMPO dataset, a collection of monthly, weekly, daily and hourly emission temporal profiles for the priority air pollutants (NO_x, SO_x, NMVOC, NH_3, CO, PM_{10}, $PM_{2.5}$) and the greenhouse gases (CO_2 and CH_4) and each of the following anthropogenic source categories: energy industry, residential combustion, manufacturing industry, road transport (exhaust and non-exhaust processes), aviation (LTO cycles) and agriculture (i.e. use of fertilizers, livestock and agricultural waste burning). Depending on the pollutant source and temporal resolution, the resulting profiles are reported as spatially invariant (i.e. a unique set of temporal weights for all the domain) or gridded values (i.e. temporal weights vary per grid cell). Multiple sources of information – including energy statistics and measured activity data, among others - and meteorology-dependent parametrizations have been collected and adapted to construct the profiles.

The CAMS-TEMPO profiles were designed to be combined with the global and regional anthropogenic emission inventories developed under the framework of Copernicus (CAMS-GLOB_ANT and CAMS-REG_AP/GHG, respectively), and to break down the original aggregated annual emissions to finer temporal resolutions (up to hourly). In order to ensure this combination, the developed temporal weight factors were constructed at a global 0.1x0.1 deg and regional 0.1x0.05 deg resolution following the domain descriptions and emission sector classification system defined in the each of the inventories.

https://doi.org/10.5194/essd-2020-175
Preprint. Discussion started: 4 August 2020

There are several features that makes the CAMS-TEMPO profiles a major step when compared to the datasets currently being used for air quality modelling under the framework of CAMS:

- Pollutant-dependency: For some sectors, profiles were computed for all species independently in order to account for the variability of the activity patterns and the specific processes that drive their release to the atmosphere. As an example, a distinction was made between the temporal distribution of traffic emissions from non-exhaust PM mainly driven by traffic activity and non-exhaust NMVOC evaporation mainly driven by outdoor temperature.
- Spatial variability: For nearly all sectors, the temporal profiles are made country or even country and region-specific in order to take into account the effects of e.g., different sociodemographic patterns and climatological conditions. For instance, differences between urban and rural traffic activity patterns are considered in the profiles constructed for road transport emissions.
- Meteorological influence: For the residential/commercial combustion, road transport and agriculture sector, the profiles were constructed using meteorology-dependent parametrizations (e.g. heating degree day, temperature effect on exhaust traffic emissions) that account for the emissions variability driven by temperature or wind speed. The resulting profiles are year-dependent and cover a timespan that goes from 2010 to 2017.

Several CAMS-TEMPO profiles are analyzed in this paper to illustrate their main characteristics and potential. Moreover, an inter-comparison exercise against independent observational datasets (e.g. real-world measurements of natural gas consumptions, emissions and pollutant concentrations) and other existing sets of temporal profiles was also performed. The comparison between CAMS-TEMPO temporal weight factors and the measurement-based profiles showed in general a high degree of correlation. Despite the scarcity of independent measurements, our comparison suggests a high level of representativeness of the developed profiles. On the other hand, the comparison against other sets of temporal profiles showed important discrepancies, especially for the traffic and agricultural sectors. This comparison highlights some shortcomings of the global and regional profiles currently used in the framework of CAMS, namely the omission of meteorological influences and the neglection of the temporal variation of emissions across sectors, species and/or countries/regions.

It is important to highlight that the continuous growth of the open data movement has been a key element for the successful development of the CAMS-TEMPO data. Services such as the European Open Data Portal (https://data.europa.eu/euodp/en/data) - and similar initiatives at the city level - or the ENTSO-E Transparency platform (ENTSO-E, 2018) are delivering very valuable data for the development of emission-related databases. Despite all the efforts, there are, however, some limitations associated to the current version of the CAMS-TEMPO profiles. First, and most importantly, the specificity of the computed profiles depends upon the degree of sectoral disaggregation used to report the original CAMS inventories. For instance, monthly profiles per industrial divisions could not be considered, since all manufacturing emissions are reported under a unique sector in both CAMS-GLOB_ANT and CAMS-REG_AP/GHG. On the

https://doi.org/10.5194/essd-2020-175
Preprint. Discussion started: 4 August 2020

other hand, the split by fuel type of traffic emissions in the CAMS-REG_AP/GHG inventory allowed to consider meteorological influences associated to e.g. CO gasoline and NO_x diesel emissions, but specific traffic activity dynamics associated to light-duty and heavy-duty vehicles could not be accounted for. A second limitation is related to the assumptions made for certain sources, mainly the residential/commercial combustion sector. The application of the Heating Degree Day approach was done considering a threshold temperature and a fraction of non-space heating activities homogenous for all the world (15.5ºC and 0.2, respectively). Several studies have highlighted that these two values can vary across regions due to changes in local climate, building characteristics and socio-demographic aspects (e.g. Grythe et al., 2019). Another important shortcoming of the current CAMS-TEMPO dataset is related to the scarcity of available information in developing countries (i.e. Africa, Latin America and Asia).

The CAMS-TEMPO dataset represents an effort to improve the temporal characterisation of emission data to be used for atmospheric chemistry modelling. Future works will include the evaluation of these temporal profiles when used for modelling activities. Through close cooperation with air quality modelers, we expect to obtain feedback on the dataset as well as suggestions for future improvements. Besides that, a number of future updates have also been identified during the present work, including:

- The extension of the year dependent temporal profiles to be in line with the current timespan considered in the CAMS-GLOB_ANT (2000-2018) and CAMS-REG_AP/GHG (2000-2017) inventories.
- The development of new temporal profiles for certain sectors/pollutants that have not currently been considered, including CH_4 emissions from agriculture (rice fields) and waste management (landfills).
- The refinement of the heating degree day approach considering region-dependent threshold temperature values.

Besides the identified updates, the investigation of monthly and seasonal changes of emissions using satellite data will be also explored in future works. Global and high-resolution observations of the atmospheric composition provided by missions such as the Copernicus Sentinel-5 Precursor (S5P) can be of great value to improve the description of the spatio-temporal distribution of emissions (Lorente et al., 2019). Finally, understanding and quantifying the impact of the current COVID-19 lockdowns upon the temporal distribution of emissions will be also an important topic to be studied.

The CAMS-TEMPO profiles are distributed free of charge through the Emissions of atmospheric Compounds and Compilation of Ancillary Data (ECCAD) system (https://eccad.aeris-data.fr/).

https://doi.org/10.5194/essd-2020-175
Preprint. Discussion started: 4 August 2020

Open Access Earth System Science Data Discussions

Appendix A

Table A1: Fixed monthly temporal profiles per domain, sector and pollutant. The definition of the sectors can be found in Table 1 and Table 2

Domain	Sector	Pollutant	1	2	3	4	5	6	7	8	9	10	11	12
CAMS-GLOB	fef	All	1.2	1.2	1.2	0.8	0.8	0.8	0.8	0.8	0.8	1.2	1.2	1.2
CAMS-GLOB	slv	All	0.95	0.96	1.02	1	1.01	1.03	1.03	1.01	1.04	1.03	1.01	0.91
CAMS-GLOB	tnr	All	1	1	1	1	1	1	1	1	1	1	1	1
CAMS-GLOB	swd	All	1	1	1	1	1	1	1	1	1	1	1	1
CAMS-GLOB	mma	PM_{10}, $PM_{2.5}$, CO, SO_x, NMVOC, CO_2, CH_4	1	1	1	1	1	1	1	1	1	1	1	1
CAMS-GLOB	agr	CH_4	1	1	1	1	1	1	1	1	1	1	1	1
CAMS-REG	GNFR_D	All	1.2	1.2	1.2	0.8	0.8	0.8	0.8	0.8	0.8	1.2	1.2	1.2
CAMS-REG	GNFR_E	All	0.95	0.96	1.02	1	1.01	1.03	1.03	1.01	1.04	1.03	1.01	0.91
CAMS-REG	GNFR_F4	NMVOC	0.74	0.69	0.74	0.84	1	1.2	1.54	1.5	1.23	1.03	0.77	0.72
CAMS-REG	GNFR_K	PM_{10}, $PM_{2.5}$, CO, SO_x, NMVOC, CO_2, CH_4	1	1	1	1	1	1	1	1	1	1	1	1
CAMS-REG	GNFR_L	CH_4	1	1	1	1	1	1	1	1	1	1	1	1
CAMS-REG	GNFR_I	All	1	1	1	1	1	1	1	1	1	1	1	1
CAMS-REG	GNFR_J	All	1	1	1	1	1	1	1	1	1	1	1	1

855

https://doi.org/10.5194/essd-2020-175
Preprint. Discussion started: 4 August 2020

Open Access Earth System Science Data Discussions

Table A2: Fixed weekly temporal profiles per domain, sector and pollutant. The definition of the sectors can be found in Table 1 and Table 2

Domain	Sector	Pollutant	1	2	3	4	5	6	7
CAMS-GLOB	ind	All	1.08	1.08	1.08	1.08	1.08	0.8	0.8
CAMS-GLOB	agr	PM_{10}, $PM_{2.5}$, CO, NO_x, NMVOC, CO_2, CH_4	1	1	1	1	1	1	1
CAMS-GLOB	fef	All	1	1	1	1	1	1	1
CAMS-GLOB	slv	All	1.2	1.2	1.2	1.2	1.2	0.5	0.5
CAMS-GLOB	tnr	All	1	1	1	1	1	1	1
CAMS-GLOB	swd	All	1	1	1	1	1	1	1
CAMS-REG	GNFR_B	All	1.08	1.08	1.08	1.08	1.08	0.8	0.8
CAMS-REG	GNFR_L	PM_{10}, $PM_{2.5}$, CO, NO_x, NMVOC, CO_2, CH_4	1	1	1	1	1	1	1
CAMS-REG	GNFR_H	All	1	1	1	1	1	1	1
CAMS-REG	GNFR_D	All	1	1	1	1	1	1	1
CAMS-REG	GNFR_E	All	1.2	1.2	1.2	1.2	1.2	0.5	0.5
CAMS-REG	GNFR_I	All	1	1	1	1	1	1	1
CAMS-REG	GNFR_J	All	1	1	1	1	1	1	1

https://doi.org/10.5194/essd-2020-175
Preprint. Discussion started: 4 August 2020

Open Access Earth System Science Data Discussions

Table A3: Fixed hourly temporal profiles per domain, sector and pollutant (Part 1: from 1 to 12h). The definition of the sectors can be found in Table 1 and Table 2.

Domain	Sector	Pollutant	1	2	3	4	5	6	7	8	9	10	11	12
CAMS-GLOB	ind	All	0.75	0.75	0.78	0.82	0.88	0.95	1.02	1.09	1.16	1.22	1.28	1.3
CAMS-GLOB	agr	NH_3, CH_4	0.6	0.6	0.6	0.6	0.6	0.65	0.75	0.9	1.1	1.35	1.45	1.6
CAMS-GLOB	agr	PM_{10}, $PM_{2.5}$, CO, SO_x, NO_x, NMVOC, CO_2	0.06	0.06	0.06	0.07	0.07	0.07	0.2	0.2	0.2	1.82	1.82	1.82
CAMS-GLOB	mma	All	0.6	0.6	0.6	0.6	0.6	0.65	0.75	0.9	1.1	1.35	1.45	1.6
CAMS-GLOB	fef	All	1	1	1	1	1	1	1	1	1	1	1	1
CAMS-GLOB	slv	All	0.5	0.35	0.2	0.1	0.1	0.2	0.75	1.25	1.4	1.5	1.5	1.5
CAMS-GLOB	tnr	All	1	1	1	1	1	1	1	1	1	1	1	1
CAMS-GLOB	swd	All	1	1	1	1	1	1	1	1	1	1	1	1
CAMS-REG	GNFR_B	All	0.75	0.75	0.78	0.82	0.88	0.95	1.02	1.09	1.16	1.22	1.28	1.3
CAMS-REG	GNFR_F4	NMVOC	0.48	0.36	0.29	0.25	0.21	0.25	0.4	0.74	1.01	1.38	1.57	1.71
CAMS-REG	GNFR_K	All	0.6	0.6	0.6	0.6	0.6	0.65	0.75	0.9	1.1	1.35	1.45	1.6
CAMS-REG	GNFR_L	NH_3, CH_4	0.6	0.6	0.6	0.6	0.6	0.65	0.75	0.9	1.1	1.35	1.45	1.6
CAMS-REG	GNFR_L	PM_{10}, $PM_{2.5}$, CO, SO_x, NO_x, NMVOC, CO_2	0.06	0.06	0.06	0.07	0.07	0.07	0.2	0.2	0.2	1.82	1.82	1.82
CAMS-REG	GNFR_H	All	0.28	0.13	0.1	0.08	0.09	0.09	0.44	0.91	1.18	1.43	1.6	1.61
CAMS-REG	GNFR_D	All	1	1	1	1	1	1	1	1	1	1	1	1
CAMS-REG	GNFR_E	All	0.5	0.35	0.2	0.1	0.1	0.2	0.75	1.25	1.4	1.5	1.5	1.5
CAMS-REG	GNFR_I	All	1	1	1	1	1	1	1	1	1	1	1	1
CAMS-REG	GNFR_J	All	1	1	1	1	1	1	1	1	1	1	1	1

https://doi.org/10.5194/essd-2020-175
Preprint. Discussion started: 4 August 2020

Open Access Earth System Science Data Discussions

Table A4: Fixed hourly temporal profiles per domain, sector and pollutant (Part 2: 13 to 24h). The definition of the sectors can be found in Table 1 and Table 2.

Domain	Sector	Pollutant	13	14	15	16	17	18	19	20	21	22	23	24
CAMS-GLOB	ind	All	1.22	1.24	1.25	1.16	1.08	1.01	0.95	0.9	0.85	0.81	0.78	0.75
CAMS-GLOB	agr	NH_3, CH_4	1.65	1.75	1.7	1.55	1.35	1.1	0.9	0.75	0.65	0.6	0.6	0.6
CAMS-GLOB	agr	PM_{10}, $PM_{2.5}$, CO, SO_x, NO_x, NMVOC, CO_2	3.39	3.39	3.39	1.68	1.68	1.68	0.56	0.56	0.56	0.22	0.22	0.22
CAMS-GLOB	mma	All	1.65	1.75	1.7	1.55	1.35	1.1	0.9	0.75	0.65	0.6	0.6	0.6
CAMS-GLOB	fef	All	1	1	1	1	1	1	1	1	1	1	1	1
CAMS-GLOB	slv	All	1.5	1.5	1.5	1.5	1.5	1.4	1.25	1.1	1	0.9	0.8	0.7
CAMS-GLOB	tnr	All	1	1	1	1	1	1	1	1	1	1	1	1
CAMS-GLOB	swd	All	1	1	1	1	1	1	1	1	1	1	1	1
CAMS-REG	GNFR_B	All	1.22	1.24	1.25	1.16	1.08	1.01	0.95	0.9	0.85	0.81	0.78	0.75
CAMS-REG	GNFR_F4	NMVOC	1.8	1.86	1.86	1.79	1.6	1.43	1.24	1.03	0.86	0.7	0.61	0.57
CAMS-REG	GNFR_K	All	1.65	1.75	1.7	1.55	1.35	1.1	0.9	0.75	0.65	0.6	0.6	0.6
CAMS-REG	GNFR_L	NH_3, CH_4	1.65	1.75	1.7	1.55	1.35	1.1	0.9	0.75	0.65	0.6	0.6	0.6
CAMS-REG	GNFR_L	PM_{10}, $PM_{2.5}$, CO, SO_x, NO_x, NMVOC, CO_2	3.39	3.39	3.39	1.68	1.68	1.68	0.56	0.56	0.56	0.22	0.22	0.22
CAMS-REG	GNFR_H	All	1.66	1.58	1.47	1.43	1.42	1.46	1.46	1.4	1.39	1.25	0.96	0.58
CAMS-REG	GNFR_D	All	1	1	1	1	1	1	1	1	1	1	1	1
CAMS-REG	GNFR_E	All	1.5	1.5	1.5	1.5	1.5	1.4	1.25	1.1	1	0.9	0.8	0.7
CAMS-REG	GNFR_I	All	1	1	1	1	1	1	1	1	1	1	1	1
CAMS-REG	GNFR_J	All	1	1	1	1	1	1	1	1	1	1	1	1

https://doi.org/10.5194/essd-2020-175
Preprint. Discussion started: 4 August 2020

875

6 Authors contribution

Marc Guevara conceived and coordinated the development of the CAMS-TEMPO profiles. Carles Tena helped constructing the CAMS-TEMPO data files. Nellie Elguindi and Claire Granier provided feedback for the construction of the global profiles and its combination with the CAMS-GLOB-ANT inventory. Hugo Denier van der Gon and Jeroen Kuenen provided feedback
880 for the construction of the European regional profiles and its combination with the CAMS-REG-AP/GHG inventory. Sabine Darras processed and prepared the CAMS-TEMPO data files to make them available through the ECCAD system. Oriol Jorba and Carlos Pérez García-Pando helped conceiving the CAMS-TEMPO dataset and supervised the work. Marc Guevara prepared the manuscript with contributions from all co-authors.

7 Acknowledgements

885 The present work was funded through the CAMS_81 (CAMS global and regional emissions) contract, coordinated by the Centre National de la Recherche Scientifique (CNRS, Claire Granier).The Copernicus Atmosphere Monitoring Service (CAMS, https://atmosphere.copernicus.eu/) is operated by the European Centre for Medium-Range Weather Forecasts on behalf of the European Commission as part of the Copernicus Programme. The study has also received support from the Ministerio de Ciencia, Innovación y Universidades (MICINN) as part of the BROWNING project RTI2018-099894-B-I00 and
890 NUTRIENT project CGL2017-88911-R. Carlos Pérez García-Pando acknowledges long-term support from the AXA Research Fund, as well as the support received through the Ramón y Cajal programme (grant RYC-2015-18690) of the MICINN. We acknowledge PRACE and RES for awarding access to MareNostrum at Barcelona Supercomputing Center. The authors are thankful to the Spanish Research Centre for Energy, Environment and Technology (CIEMAT) for sharing the databases of power plant emissions.

8 Competing interests

895

The authors declare that they have no conflict of interest.

https://doi.org/10.5194/essd-2020-175
Preprint. Discussion started: 4 August 2020

References

AB: Barcelona City Council. Mobility data 2015. Available at: https://www.barcelona.cat/mobilitat/sites/default/files/DB_2015.pdf (last accessed January 2019), 2017.

Athanasopoulou, E., Speyer, O., Brunner, D., Vogel, H., Vogel, B., Mihalopoulos, N., and Gerasopoulos, E.: Changes in domestic heating fuel use in Greece: effects on atmospheric chemistry and radiation, Atmos. Chem. Phys., 17, 10597-10618, https://doi.org/10.5194/acp-17-10597-2017, 2017.

Backes, A., Aulinger, A., Bieser, J., Matthias, V., and Quante, M.: Ammonia emissions in Europe, part I: Development of a dynamical ammonia emission inventory, Atmos. Environ., 131, 55–66, http://dx.doi.org/10.1016/j.atmosenv.2016.01.041, 2016.

BASt: Federal Highway Research Institute. Automatic counting stations on highways and federal highways. Available at: https://www.bast.de/BASt_2017/DE/Verkehrstechnik/Fachthemen/v2-verkehrszaehlung/zaehl_node.html (last accessed April 2018), 2018.

Bieser, J., Aulinger, A., Matthias, V., Quante, M., and Builtjes, P.: SMOKE for Europe – adaptation, modification and evaluation of a comprehensive emission model for Europe, Geosci. Model Dev., 4, 47–68, https://doi.org/10.5194/gmd-4-47-2011, 2011.

Bonjour, S., Adair-Rohani, H., Wolf, J., Bruce, N. G., Mehta, S., Pruss-Ustun, A., Lahiff, M., Rehfuess, E. A., Mishra, V., and Smith, K. R.: Solid fuel use for household cooking: country and regional estimates for, Environ. Health Persp., 121, 784–790, https://doi.org/10.1289/ehp.1205987, 2013.

Borge, R., Lumbreras, J., and Rodríguez, E.: Development of a high-resolution emission inventory for Spain using the SMOKE modelling system: A case study for the years 2000 and 2010, Environ. Model. Softw., 23, 1026-1044, https://doi.org/10.1016/j.envsoft.2007.11.002, 2008.

Cai, H., and Xie, S.: Traffic-related air pollution modeling during the 2008 Beijing olympic games: the effects of an odd-even day traffic restriction scheme, Sci Total Environ, 409, 1935-1948, https://doi.org/10.1016/j.scitotenv.2011.01.025, 2011.

Copernicus Climate Change Service (C3S): ERA5: Fifth generation of ECMWF atmospheric reanalyses of the global climate. Copernicus Climate Change Service Climate Data Store (CDS), Available at:. https://cds.climate.copernicus.eu/cdsapp#!/home , (last accessed, July 2019) 2017.

Copenhagen data: Copenhagen city open data portal. Permanent Traffic Counting. Available at: https://portal.opendata.dk/dataset/faste-trafiktaellinger (last accessed February 2018), 2018.

Crippa, M., Solazzo, E., Huang, G., Guizzardi, D., Koffi, E., Muntean, M., Schieberle, C., Friedrich, R., and Janssens-Maenhout, G.: High resolution temporal profiles in the Emissions Database for Global Atmospheric Research. Scientific Data 7, 121, doi:10.1038/s41597-020-0462-2, 2020.

Denier van der Gon, H. A. C., Hendriks, C., Kuenen, J., Segers, A., and Visschedijk, A. J. H.: Description of current temporal emission patterns and sensitivity of predicted AQ for temporal emission patterns, EU FP7 MACC deliverable report D_D-EMIS_1.3, 2011.

https://doi.org/10.5194/essd-2020-175
Preprint. Discussion started: 4 August 2020

Ebel, A., Friedrich, R., and Rodhe, H.: GENEMIS: Assessment, Improvement, and Temporal and Spatial Disaggregation of European Emission Data, in Tropospheric Modelling and Emission Estimation: Chemical Transport and Emission Modelling on Regional, Global and Urban Scales, edited by: Ebel, A., Friedrich, R., and Rodhe, H., 181–214, Springer Berlin Heidelberg, Berlin, Heidelberg, https://doi.org/10.1007/978-3-662-03470-5_6, 1997.

EMEP/EEA: Air pollutant emission inventory guidebook 2016. Technical guidance to prepare national emission inventories.

EMEP/CEIP: Present state of emission data. Available at: http://www.ceip.at/webdab_emepdatabase/reported_emissiondata/ (last accessed, March 2020), 2019.

EEA: Report No 21/2016. Available at: https://www.eea.europa.eu/publications/emep-eea-guidebook-2016 (last accessed, July 2019), 2016.

EEA: Download service of air quality data. Available at: http://discomap.eea.europa.eu/map/fme/AirQualityExport.htm (last accessed January 2019), 2019.

Eurostat: Energy consumption in households. Available at: https://ec.europa.eu/eurostat/statistics-explained/index.php/Energy_consumption_in_households (last accessed, May 2018), 2018.

Eurostat: Airport traffic data by reporting airport and airlines. Available at: https://ec.europa.eu/eurostat/web/products-datasets/product?code=avia_tf_apal (last accessed, March 2020), 2019.

ENTSO-E: Transparency Platform. Available at: https://transparency.entsoe.eu/ (last accessed, May 2018), 2018.

ENTSOG: Transparency platform. Available at: https://transparency.entsog.eu/#/map (last accessed, March 2020), 2020.

Fameli, K.M., and Assimakopoulos, V.D.: Development of a road transport emission inventory for Greece and the Greater Athens Area: effects of important parameters. Sci. Total Environ., 505, 770-786, https://doi.org/10.1016/j.scitotenv.2014.10.015, 2015.

Finstad, A., Flugsrud, K., Haakonsen, G., Aasestad, K.: Wood consumption, fire habits and particulate matter. Results from Folke and housing census 2001, Living Conditions Survey 2002 and Survey of wood consumption and firing habits in Oslo 2002Statistics Norway. Rapporter 2004/5 (in Norwegian), 2004.

Florczyk, A.J., Corbane, C., Ehrlich, D., Freire, S., Kemper, T., Maffenini, L., Melchiorri, M., Pesaresi, M., Politis, P., Schiavina, M., Sabo, F., and Zanchetta, L.: GHSL Data Package 2019,EUR 29788EN, Publications Office of the European Union, Luxembourg, 2019, ISBN 978-92-76-08725-0, doi:10.2760/062975, JRC117104, 2019.

Friedrich, R. and Reis, S. (Eds.): Emissions of Air Pollutants – Measurements, Calculation, Uncertainties – Results from the EUROTRAC-2 Subproject GENEMIS, Springer Publishers, Berlin, Heidelberg, Germany, 2004.

GADM: Database of Global Administrative Areas. Available at: www.gadm.org (last accessed, July 2020), 2020.

Galmarini, S., Koffi, B., Solazzo, E., Keating, T., Hogrefe, C., Schulz, M., Benedictow, A., Griesfeller, J. J., Janssens-Maenhout, G., Carmichael, G., Fu, J., and Dentener, F.: Technical note: Coordination and harmonization of the multi-scale, multi-model activities HTAP2, AQMEII3, and MICS-Asia3: simulations, emission inventories, boundary conditions, and model output formats, Atmos. Chem. Phys., 17, 1543–1555, https://doi.org/10.5194/acp-17-1543-2017, 2017.

https://doi.org/10.5194/essd-2020-175
Preprint. Discussion started: 4 August 2020

GovUK: Road traffic statistics information. Available at: https://www.gov.uk/government/collections/road-traffic-statistics (last accessed March 2018), 2018.

Grange, S. K., Farren, N. J., Vaughan, A. R., Rose, R. A., and Carslaw, D. C.: Strong Temperature Dependence for LightDuty Diesel Vehicle NOx Emissions, Environ. Sci. Technol., 53, 6587–6596, https://doi.org/10.1021/acs.est.9b01024, 2019.

Granier, C., Bessagnet, B., Bond, T., D'Angiola, A., van der Gon, H. D., Frost, G. J., Heil, A., Kaiser, J. W., Kinne, S., Klimont, Z., Kloster, S., Lamarque, J. F., Liousse, C., Masui, T., Meleux, F., Mieville, A., Ohara, T., Raut, J. C., Riahi, K., Schultz, M.G., Smith, S. J., Thompson, A., van Aardenne, J., van der Werf, G. R., and van Vuuren, D. P.: Evolution of anthropogenic and biomass burning emissions of air pollutants at global and regional scales during the 1980-2010 period, Clim. Change, 109, 163–190, doi:10.1007/s10584-011-0154-1, 2011.

Granier, C., Darras, S., Denier van der Gon, H. A. C., Doubalova, J., Elguindi, N., Galle, B., Gauss, M., Guevara, M., Jalkanen, J.-P., Kuenen, J., Liousse, C., Quack, B., Simpson, D., and Sindelarova, K.: The Copernicus Atmosphere Monitoring Service global and regional emissions (April 2019 version), Copernicus Atmosphere Monitoring Service (CAMS) report, 2019, https://doi.org/10.24380/d0bn-kx16, 2019.

Gröndahl, T., Makkonen J., Myllynen M., Niemi J.,Tuomi S.: Use of fireplaces and discharges from small houses in the Helsinki metropolitan area. HSY publications. Available at: https://www.hsy.fi/sites/Esitteet/EsitteetKatalogi/Raportit/Pienpolttoraportti_LR.pdf (last accessed, May 2018), 2010.

Grythe, H., Lopez-Aparicio, S., Vogt, M., Vo Thanh, D., Hak, C., Halse, A. K., Hamer, P., and Sousa Santos, G.: The MetVed model: development and evaluation of emissions from residential wood combustion at high spatio-temporal resolution in Norway, Atmos. Chem. Phys., 19, 10217–10237, https://doi.org/10.5194/acp-19-10217-2019, 2019.

Guevara, M., Jorba, O., Tena, C., Denier van der Gon, H., Kuenen, J., Elguindi, N., Darras, S., Granier, C., and Pérez García-Pando, C.: Copernicus Atmosphere Monitoring Service TEMPOral profiles for the Global domain version 2.1 (CAMS-GLOB-TEMPOv2.1), Copernicus Atmosphere Monitoring Service [publisher], ECCAD [distributor], https://doi.org/10.24380/ks45-9147, 2020a.

Guevara, M., Jorba, O., Tena, C., Denier van der Gon, H., Kuenen, J., Elguindi, N., Darras, S., Granier, C., and Pérez García-Pando, C.: Copernicus Atmosphere Monitoring Service TEMPOral profiles for the regional European domain version 2.1 (CAMS-REG-TEMPOv2.1), Copernicus Atmosphere Monitoring Service [publisher], ECCAD [distributor], https://doi.org/10.24380/1cx4-zy68, 2020b.

Guevara, M., Tena, C., Porquet, M., Jorba, O., and Pérez García-Pando, C.: HERMESv3, a stand-alone multi-scale atmospheric emission modelling framework – Part 2: The bottom–up module, Geosci. Model Dev., 13, 873–903, https://doi.org/10.5194/gmd-13-873-2020, 2020c.

Gurney, K. R., Patarasuk, R., Liang, J., Song, Y., O'Keeffe, D., Rao, P., Whetstone, J. R., Duren, R. M., Eldering, A., and Miller, C.: The Hestia fossil fuel CO2 emissions data product for the Los Angeles megacity (Hestia-LA), Earth Syst. Sci. Data, 11, 1309–1335, https://doi.org/10.5194/essd-11-1309-2019, 2019.

https://doi.org/10.5194/essd-2020-175
Preprint. Discussion started: 4 August 2020

Gyldenkærne, S., Skjøth, C.A, Hertel, O., and Ellermann, T.: A dynamical ammonia emission parameterization for use in air pollution models, J. Geophys. Res., 110, D07108, doi:10.1029/2004JD005459, 2005.

Hirth, L., Mühlenpfordt, J., and Bulkeley, M.: The ENTSO-E Transparency Platform – A review of Europe's most ambitious electricity data platform, Appl. Energy, 225, 1054-1067, https://doi.org/10.1016/j.apenergy.2018.04.048, 2018.

IEA: Electricity Statistics. Available at: http://www.iea.org/statistics/monthlystatistics/monthlyelectricitystatistics/ (last accessed, May 2018), 2018.

INE. Spanish Statistical Office. Industrial production. Available at: https://www.ine.es/en/prensa/ipi_prensa_en.htm (last accessed, May 2018), 2018.

IPCC: 2006 IPCC Guidelines for National Greenhouse Gas Inventories, Prepared by the National Greenhouse Gas Inventories Programme, Eggleston H.S., Buendia L., Miwa K., Ngara T. and Tanabe K. (eds). Published: IGES, Japan, 2006.

ISTAT. Italian National Institute of Statistics. Industrial production. Available at: https://www.istat.it/en/archive/industrial+production (last accessed, June 2018), 2018.

James, K.M., Blunden, J., Rumsey, I.C., and Aneja, V.P.: Characterizing ammonia emissions from a commercial mechanically ventilated swine finishing facility and an anaerobic waste lagoon in North Carolina, Atmos. Pollut. Res., 3, 279–288, https://doi.org/10.5094/APR.2012.031, 2012.

Janssens-Maenhout, G., Crippa, M., Guizzardi, D., Muntean, M., Schaaf, E., Dentener, F., Bergamaschi, P., Pagliari, V., Olivier, J. G. J., Peters, J. A. H. W., van Aardenne, J. A., Monni, S., Doering, U., Petrescu, A. M. R., Solazzo, E., and Oreggioni, G. D.: EDGAR v4.3.2 Global Atlas of the three major greenhouse gas emissions for the period 1970–2012, Earth Syst. Sci. Data, 11, 959–1002, https://doi.org/10.5194/essd-11-959-2019, 2019.

Keller, M., Hausberger, S., Matzer, C., Wuthrich, P., and Notter, B.: HBEFA version 3.3. Background documentation. Available at: www.umweltbundesamt.de/sites/default/files/medien/2546/dokumente/hbefa33_documentation_20170425.pdf (last accessed, March 2020), 2017.

Klimont, Z., Kupiainen, K., Heyes, C., Purohit, P., Cofala, J., Rafaj, P., Borken-Kleefeld, J., and Schöpp, W., 2017. Global anthropogenic emissions of particulate matter including black carbon, Atmos. Chem. Phys., 17, 8681-8723, https://doi.org/10.5194/acp-17-8681-2017.

Kuenen, J. J. P., Visschedijk, A. J. H., Jozwicka, M., and Denier van der Gon, H. A. C.: TNO-MACC_II emission inventory; a multi-year (2003–2009) consistent high-resolution European emission inventory for air quality modelling, Atmos. Chem. Phys., 14, 10963–10976, https://doi.org/10.5194/acp-14-10963-2014, 2014.

Li, M., Zhang, Q., Kurokawa, J.-I., Woo, J.-H., He, K., Lu, Z., Ohara, T., Song, Y., Streets, D. G., Carmichael, G. R., Cheng, Y., Hong, C., Huo, H., Jiang, X., Kang, S., Liu, F., Su, H., and Zheng, B.: MIX: a mosaic Asian anthropogenic emission inventory under the international collaboration framework of the MICS-Asia and HTAP, Atmos. Chem. Phys., 17, 935-963, https://doi.org/10.5194/acp-17-935-2017, 2017.

https://doi.org/10.5194/essd-2020-175
Preprint. Discussion started: 4 August 2020

Lorente, A., Boersma, K., Eskes, H., Veefkind, J. P., Van Geffen, J. H. G. M., De Zeeuw, M., Denier van der Gon, H., Beirle, S., and Krol, M. C.: Quantification of nitrogen oxides emissions from build-up of pollution over Paris with TROPOMI, Sci. Rep., 9, 20033, https://doi.org/10.1038/s41598-019-56428-5, 2019.

Madrid data: Madrid city open data portal. Traffic. Historic traffic data since 2013. Available at: https://datos.madrid.es/sites/v/index.jsp?vgnextoid=33cb30c367e78410VgnVCM1000000b205a0aRCRD&vgnextchannel=374512b9ace9f310VgnVCM100000171f5a0aRCRD (last accessed April 2018), 2018.

Makonin, S., Ellert, B., Bajic, I.V., and Popowich, F.: AMPds2-Almanac of Minutely Power dataset: Electricity, water, and natural gas consumption of a residential house in Canada from 2012 to 2014. Sci. Data, 3, doi:10.1038/sdata.2016.37, 2016.

Mareckova, K., Wankmueller, R., Moosmann, L., and Pinterits, M.: Inventory Review 2013: Re- view of Emission Data reported under the LRTAP Convention and NEC Directive, Stage 1 and 2 review, Status of Gridded Data and LPS Data, STATUS Report 1/2013, Umweltbundesamt GmbH, Vienna, Austria, 2013

Mareckova, K., Pinterits, M., Ullrich, B., Wankmueller, R., and Mandl, N.: Inventory review 2017. Review of emission data reported under the LRTAP Convention and the NEC Directive Stage 1 and 2 review, Status of gridded and LPS data, Technical Report CEIP 2/2017, Umweltbundesamt GmbH, Vienna, 2017.

Markakis, K., Poupkou, A., Melas, D., Tzoumaka, P., and Petrakakis, M.: A computational approach based on GIS technology for the development of an anthropogenic emission inventory of gaseous pollutants in Greece, Water Air Soil Pollut., 207, 157-180, https://doi.org/10.1007/s11270-009-0126-5, 2010.

MBS: Monthly Bulletin of Statistics Online. Available at: https://unstats.un.org/unsd/mbs/ (last accessed, March 2018), 2018.

McDonald, B. C., McBride, Z. C., Martin, E. W., and Harley, R.A.: High resolution mapping of motor vehicle carbon dioxide emissions, J. Geophys. Res. Atmos., 119, 5283–5298, doi:10.1002/ 2013JD021219, 2014.

Melbourne data: Melbourne's Open Data Platform. Traffic Count Vehicle Classification 2014 – 2017. Available at: https://data.melbourne.vic.gov.au/Transport-Movement/Traffic-Count-Vehicle-Classification-2014-2017/qksr-hqee (last accessed January 2019), 2019.

Menut, L., Goussebaile, A., Bessagnet, B., Khvorostiyanov, D., and Ung, A.: Impact of realistic hourly emissions profiles on air pollutants concentrations modelled with CHIMERE, Atmos. Environ., 49, 233–244, https://doi.org/10.1016/j.atmosenv.2011.11.057, 2012.

Milano data: Milano city open data portal. Area C traffic reporting. Available at: https://areac.amat-mi.it/it/areac/ (last accessed March 2018), 2018.

Mu, M., Randerson, J. T., van der Werf, G. R., Giglio, L., Kasibhatla, P., Morton, D., Collatz, G. J., DeFries, R. S., Hyer, E. J., Prins, E. M., Griffith, D. W. T., Wunch, D., Toon, G. C., Sherlock, V., and Wennberg, P. O.: Daily and 3-hourly variability in global fire emissions and consequences for atmospheric model predictions of carbon monoxide, J. Geophys. Res.-Atmos., 116, D24303, doi: 10.1029/2011JD016245, 2010.

https://doi.org/10.5194/essd-2020-175
Preprint. Discussion started: 4 August 2020

Mues, A., Kuenen, J., Hendriks, C., Manders, A., Segers, A., Scholz, Y., Hueglin, C., Builtjes, P., and Schaap, M.: Sensitivity of air pollution simulations with LOTOS-EUROS to the temporal distribution of anthropogenic emissions, Atmos. Chem. Phys., 14, 939-955, https://doi.org/10.5194/acp-14-939-2014, 2014.

MWDB2: Micro World Data Bank 2. Available at: http://microworld-db-2.sourceforge.net/ (last accessed, July 2020), 2011.

Nassar, R., Napier-Linton, L., Gurney, K. R., Andres, R. J., Oda, T., Vogel, F. R. and Deng, F.: Improving the temporal and spatial distribution of CO2 emissions from global fossil fuel emission data sets, J. Geophys. Res., 118(2), 917–933, doi:10.1029/2012jd018196, 2013.

New York City data: New York city open data portal. Traffic Volume Counts (2014-2018). Available at: https://data.cityofnewyork.us/Transportation/Traffic-Volume-Counts-2014-2018-/ertz-hr4r (last accessed January 2019), 2019.

Oda, T., Maksyutov, S., and Andres, R. J.: The Open-source Data Inventory for Anthropogenic CO2, version 2016 (ODIAC2016): a global monthly fossil fuel CO2 gridded emissions data product for tracer transport simulations and surface flux inversions, Earth Syst. Sci. Data, 10, 87–107, https://doi.org/10.5194/essd-10-87-2018, 2018.

ONS. Office for National Statistics. Index of production. Available at: https://www.ons.gov.uk/economy/economicoutputandproductivity/output/bulletins/indexofproduction/previousReleases (last accessed May 2018), 2018.

Paris data: Paris city open data portal. Traffic data from permanent sensors. Available at: https://opendata.paris.fr/explore/dataset/comptages-routiers-permanents/information/ (last accessed March 2018), 2018.

Paulot, F., Jacob, D. J., Pinder, R. W., Bash, J. O., Travis, K., and Henze, D. K.: Ammonia emissions in the United States, European Union, and China derived by high resolution inversion of ammonium wet deposition data: interpretation with a new agricultural emissions inventory (MASAGE_NH3), J. Geophys. Res.-Atmos., 119, 4343–4364, https://doi.org/10.1002/2013JD021130, 2014.

Pesaresi, M., Florczyk, A., Schiavina, M., Melchiorri, M., and Maffenini, L.: GHS settlement grid, updated and refined REGIO model 2014 in application to GHS-BUILT R2018A and GHS-POP R2019A, multitemporal (1975-1990-2000-2015), R2019A. European Commission, Joint Research Centre (JRC) [Dataset] doi:10.2905/42E8BE89-54FF-464E-BE7B-BF9E64DA5218 PID: http://data.europa.eu/89h/42e8be89-54ff-464e-be7b-bf9e64da5218, 2019.

Pham, T.B.T, Manomaiphiboon, K., and Vongmahadlek, C.: Development of an inventory and temporal allocation profiles of emissions from power plants and industrial facilities in Thailand, Sci. Total Environ., 397, 103-118, https://doi.org/10.1016/j.scitotenv.2008.01.066, 2008.

Quayle, R.G., and Diaz, H.F.: Heating degree day data applied to residential heating energy consumption. J. Appl. Meteorol. 19(3): 241–246, https://doi.org/10.1175/1520-0450(1980)019<0241:HDDDAT>2.0.CO;2, 1980.

Reis, S., Skjøth, A.C., Vieno, M., Geels, C., Steinle, S., Lang, M., and Sutton, M.A.: Why time and space matters-arguments for the improvement of temporal emission profiles for atmospheric dispersion modeling of air pollutant emissions. In:

https://doi.org/10.5194/essd-2020-175
Preprint. Discussion started: 4 August 2020

MODSIM 2011-19th International Congress on Modelling and Simulation Sustaining Our Future: Understanding and Living with Uncertainty,1817-1823, 2011.

Simpson, D., Benedictow, A., Berge, H., Bergström, R., Emberson, L. D., Fagerli, H., Flechard, C. R., Hayman, G. D., Gauss, M., Jonson, J. E., Jenkin, M. E., Nyíri, A., Richter, C., Semeena, V. S., Tsyro, S., Tuovinen, J.-P., Valdebenito, Á., and Wind, P., 2012. The EMEP MSC-W chemical transport model – technical description, Atmos. Chem. Phys., 12, 7825-7865, https://doi.org/10.5194/acp-12-7825-2012.

Skjøth, C. A., Geels, C., Berge, H., Gyldenkærne, S., Fagerli, H., Ellermann, T., Frohn, L. M., Christensen, J., Hansen, K. M., Hansen, K., and Hertel, O., 2011. Spatial and temporal variations in ammonia emissions – a freely accessible model code for Europe, Atmos. Chem. Phys., 11, 5221-5236, https://doi.org/10.5194/acp-11-5221-2011.

Spinoni, Vogt, J., and Barbosa, P., European degree-day climatologies and trends for the period 1951–2011, Int. J. Climatol. 35: 25–36, https://doi.org/10.1002/joc.3959, 2015.

SSB. StatBank Norway. Index of industrial production. Available at: https://www.ssb.no/en/pii/ (last accessed July 2018), 2018.

Stohl, A., Klimont, Z., Eckhardt, S., Kupiainen, K., Shevchenko, V. P., Kopeikin, V. M., and Novigatsky, A. N.: Black carbon in the Arctic: the underestimated role of gas flaring and residential combustion emissions, Atmos. Chem. Phys., 13, 8833–8855, https://doi.org/10.5194/acp-13-8833-2013, 2013.

Super, I., Dellaert, S. N. C., Visschedijk, A. J. H., and Denier van der Gon, H. A. C.: Uncertainty analysis of a European high-resolution emission inventory of CO2 and CO to support inverse modelling and network design, Atmos. Chem. Phys., 20, 1795–1816, https://doi.org/10.5194/acp-20-1795-2020, 2020.

Terrenoire, E., Bessagnet, B., Rouïl, L., Tognet, F., Pirovano, G., Létinois, L., Beauchamp, M., Colette, A., Thunis, P., Amann, M., and Menut, L.: High-resolution air quality simulation over Europe with the chemistry transport model CHIMERE, Geosci. Model Dev., 8, 21-42, https://doi.org/10.5194/gmd-8-21-2015, 2015.

TfNSW: Transport for New South Wales Open Data. NSW Roads Traffic Volume Counts. Available at: https://opendata.transport.nsw.gov.au/dataset/nsw-roads-traffic-volume-counts-api (last accessed January 2019), 2019.

Thiruchittampalam, B., 2014: Entwicklung und Anwendung von Methoden und Modellen zur Berechnung von räumlich und zeitlich hochaufgelösten Emissionen in Europa. Forschungsbericht Band 118. Institute of Energy Economics and Rational Energy Use, University of Stuttgart, Germany.

Unal, A., Hu, Y., Chang, M. E., Talat Odman, M., and Russell, A. G.: Airport related emissions and impacts on air quality: application to the Atlanta International Airport, Atmos. Environ., 39, 5787–5798, doi:10.1016/j.atmosenv.2005.05.051, 2005.

US EPA: Emission Adjustments for Temperature, Humidity, Air Conditioning, and Inspection and Maintenance for On-road Vehicles in MOVES2014. EPA-420-R-15-020. Available at: https://nepis.epa.gov/Exe/ZyPDF.cgi?Dockey=P100NOEM.pdf (last accessed, March 2020), 2015.

US EPA: Emissions Modeling platforms. Available at: https://www.epa.gov/air-emissions-modeling/emissions-modeling-platforms (last accessed, March 2020), 2019a.

https://doi.org/10.5194/essd-2020-175
Preprint. Discussion started: 4 August 2020

US EPA: Environmental Protection Agency. 2014 version 7.1 NEI Emissions Modeling Platform, https://doi.org/10.15139/S3/1VJGUY, UNC Dataverse, V2, 2019b.

Utrecht data: The Netherlands data platform. Utrecht traffic counts 2014. Available at: https://ckan.dataplatform.nl/en/dataset/verkeer-tellingen-verkeerslichten-2014 (last accessed March 2018), 2018.

VLB: Berlin Traffic Control. Average daily traffic volume 2014. Available at: https://www.stadtentwicklung.berlin.de/umwelt/umweltatlas/edd701_03.htm (last accessed October 2018), 2018.

Walker, J. T., Jones, M. R., Bash, J. O., Myles, L., Meyers, T., Schwede, D., Herrick, J., Nemitz, E., and Robarge, W.: Processes of ammonia air–surface exchange in a fertilized Zea mays canopy, Biogeosciences, 10, 981-998, https://doi.org/10.5194/bg-10-981-2013, 2013.

Warner, J. X., Dickerson, R. R., Wei, Z., Strow, L. L., Wang, Y., and Liang, Q.: Increased atmospheric ammonia over the world's major agricultural areas detected from space, Geophys. Res. Lett., 44, 2875–2884, https://doi.org/10.1002/2016GL072305, 2017.

Werner, M., Ambelas Skjøth, C., Kryza, M., and Dore, A. J.: Understanding emissions of ammonia from buildings and the application of fertilizers: an example from Poland, Biogeosciences, 12, 3623–3638, https://doi.org/10.5194/bg-12-3623-2015, 2015.

World Bank: World Economic Situation and Prospects. Country Classification. Available at: https://www.un.org/en/development/desa/policy/wesp/wesp_current/2014wesp_country_classification.pdf (last accessed October 2018), 2014.

Zhang, L., Chen, Y., Zhao, Y., Henze, D. K., Zhu, L., Song, Y., Paulot, F., Liu, X., Pan, Y., Lin, Y., and Huang, B.: Agricultural ammonia emissions in China: reconciling bottom-up and top-down estimates, Atmos. Chem. Phys., 18, 339-355, https://doi.org/10.5194/acp-18-339-2018, 2018.

Zheng, J., Zhang, L., Che, W., Zheng, Z., and Yin, S.: A highly resolved temporal and spatial air pollutant emission inventory for the Pearl River Delta region, China and its uncertainty assessment. Atmos. Env., 43, 5112–5122, https://doi.org/10.1016/j.atmosenv.2009.04.060, 2009.

Zheng, B., Huo, H., Zhang, Q., Yao, Z. L., Wang, X. T., Yang, X. F., Liu, H., and He, K. B.: High-resolution mapping of vehicle emissions in China in 2008, Atmos. Chem. Phys., 14, 9787-9805, https://doi.org/10.5194/acp-14-9787-2014, 2014

Zhou, Y., Jiao, Y., Lang, J., Chen, D., Huang, C., Wei, P., Li, S., and Cheng, S.: Improved estimation of air pollutant emissions from landing and takeoff cycles of civil aircraft in China, Environmental Pollution, 249, 463-471, https://doi.org/10.1016/j.envpol.2019.03.088, 2019.

https://doi.org/10.5194/essd-2020-175
Preprint. Discussion started: 4 August 2020

Open Access Earth System Science Data Discussions

Table 1: Main characteristics of the CAMS global temporal profiles (CAMS-GLOB-TEMPO) reported by sector and temporal resolution (monthly, daily, weekly, hourly). Per country: indicates that the profiles vary per country; per pollutant: indicates that the profiles vary per pollutant; per region: indicates that the profiles vary per grid cell within a country; fixed: indicates that the profiles are spatially invariant. The symbol "-" denotes that no profile is proposed.

Sector	Description	Monthly (∑=12)	Daily (∑=365/366)[1]	Weekly (∑=7)	Hourly (∑=24)
ene	Power generation (power and heat plants, refineries, others)	(per country, pollutant)	-	(per country, pollutant)	(per country, pollutant)
ind	Industrial process	(per country)	-	(fixed)[2]	(fixed)[2]
res	Other stationay combustion (residential, commercial, agriculture, others)	(per region, year)	(per region, year)	(fixed)[2]	(per region, pollutant)
fef	Fugitives	(fixed)[2]	-	(fixed)[2]	(fixed)[2]
slv	Solvents	(fixed)[2]	-	(fixed)[2]	(fixed)[2]
tro	Road transportation	(per region)	-	(per region)	(per day type)
shp	Ships	(fixed)[2]	-	(fixed)[2]	(fixed)[2]
tnr	Off road transportation (airports, agricultural and construction machinery, others)	(fixed)[2]	-	(fixed)[2]	(fixed)[2]
swd	Solid waste and waste water	(fixed)[2]	-	(fixed)[2]	(fixed)[2]
mma	Agriculture (livestock)	(per region, year for NH_3 and NO_x; fixed for others)	(per region, year for NH_3 and NO_x)	(fixed)[2]	(fixed)[2]
agr	Agriculture (fertilizers and agricultural waste burning)	(per region)	(per region, year for NH_3)	(fixed)[2]	(fixed, per pollutant)

[1] Leap or non-leap years
[2] Same profiles as the ones reported by the TNO dataset (Denier van der Gon et al., 2011)

https://doi.org/10.5194/essd-2020-175
Preprint. Discussion started: 4 August 2020

Open Access Earth System Science Data Discussions

Table 2: Main characteristics of the CAMS regional temporal profiles (CAMS-REG-TEMPO) reported by sector and temporal resolution (monthly, daily, weekly, hourly). Per country: indicates that the profiles vary per country; per pollutant: indicates that the profiles vary per pollutant; per region: indicates that the profiles vary per grid cell within a country; fixed: indicates that the profiles are spatially invariant. The symbol "-" denotes that no profile is proposed.

Sector	Description	Monthly (∑=12)	Daily (∑=365/366)[1]	Weekly (∑=7)	Hourly (∑=24)
GNFR_A	Public Power (power and heat plants)	(per country, pollutant)	-	(per country, pollutant)	(per country, pollutant)
GNFR_B	Industry	(per country)	-	(fixed)[2]	(fixed)[2]
GNFR_C	Other stationay combustion (residential, commercial, agriculture, others)	(per region, year)	(per region, year)	(fixed)[2]	(per region, pollutant)
GNFR_D	Fugitive	(fixed)[2]	-	(fixed)[2]	(fixed)[2]
GNFR_E	Solvents	(fixed)[2]	-	(fixed)[2]	(fixed)[2]
GNFR_F1	Road transport exhaust gasoline	(per year, region for CO and NMVOC; per region for others)	-	(per region)	(per region, day type)
GNFR_2	Road transport exhaust diesel	(per year, region for NO_x; per region for others)	-	(per region)	(per region, day type)
GNFR_F3	Road transport exhaust LPG	(per region)	-	(per region)	(per region, day type)
GNFR_F4	Road transport non-exhaust (wear and evaporative)	(per region for PM; fixed for NMVOC)	-	(per region for PM; fixed for NMVOC)	(per region, day type for PM; fixed for NMVOC)
GNFR_G	Shipping	(fixed)[2]	-	(fixed)[2]	(fixed)[2]
GNFR_H	Aviation	(per country)	-	(fixed)[2]	(fixed)
GNFR_I	Off road transport (agricultural, and construction machinery, others)	(fixed)[2]	-	(fixed)[2]	(fixed)[2]
GNFR_I	Waste management	(fixed)[2]	-	(fixed)[2]	(fixed)[2]
GNFR_K	Agriculture (livestock)	(per region, year for NH_3 and NO_x; fixed for others)	(per region, year for NH_3 and NO_x)	(fixed)[2]	(fixed)[2]
GNFR_L	Agriculture (fertilizers, agricultural waste burning)	(per region)	(per region, year for NH_3)	(fixed)[2]	(fixed, per pollutant)

[1] Leap or non-leap years
[2] Same profiles as the ones reported by the TNO dataset (Denier van der Gon et al., 2011)

https://doi.org/10.5194/essd-2020-175
Preprint. Discussion started: 4 August 2020

Open Access Earth System Science Data Discussions

Table 3: Emission factors [kg·TJ^{-1}] related to the energy industry per fuel type and pollutant. Values obtained from the EMEP/EEA 2016 emission inventory guidebook for the priority air pollutants (1.A.1 Energy industries, Table 3-2, 3-3, 3-4, 3-5 and 3-7) and from the IPPC guidelines (Volume 2: Energy, Table 2.2) for greenhouse gases.

Fuel / EF [kg·TJ^{-1}]	NO_x	SO_x	CO	NMVOC	PM_{10}	$PM_{2.5}$	CO_2	CH_4
Hard Coal	209	820	8.7	1.0	7.7	3.4	98,300	1
Brown Coal (Lignite)	247	1680	8.7	1.4	7.9	3.2	101,000	1
Gaseous fuels (natural gas)	89	0.281	39	2.6	0.89	0.89	56,100	1
Heavy Fuel Oil	142	495	15.1	2.3	25.2	19.3	77,400	1
Biomass	81	10.8	90	7.31	155	133	112,000	30

https://doi.org/10.5194/essd-2020-175
Preprint. Discussion started: 4 August 2020

Open Access Earth System Science Data Discussions

Table 4: Share of final energy consumption in the residential sector by fuel and type of end-use in Europe (Eurostat, 2018)

Fuel	Space heating	Water heating	Cooking	Other end uses
Gas	77.7%	17.2%	5.1%	-
Solid fuels (coal products)	90.7%	8.2%	1.1%	-
Petroleum products (LPG, fuel oil)	81.1%	12.9%	6.0%	0.1%
Renewables and wastes (solid biofuels)	89.1%	8.8%	1.7%	0.4%
All	**81.8%**	**13.9%**	**4.2%**	**0.1%**

https://doi.org/10.5194/essd-2020-175
Preprint. Discussion started: 4 August 2020

Open Access Earth System Science Data Discussions

Table 5: List of traffic activity datasets and corresponding sources of information compiled

Dataset	Description	Source of Information
Paris city	Hourly traffic counts registered at the permanent stations for the years 2013 - 2017	Paris data (2018)
Madrid city	Hourly traffic counts registered at the permanent stations for the years 2013 - 2017	Madrid data (2018)
Barcelona city	Hourly traffic counts registered at the permanent stations for the year 2015	Courtesy from Barcelona city council
Valencia city	Hourly traffic counts registered at the permanent stations for the year 2009	Courtesy from Valencia city council
Milano city	Hourly traffic counts registered at the permanent stations for the year 2013	Milano data (2018)
Utrecht city	Hourly traffic counts registered at the permanent stations for the years 2014-2015	Utrecht data (2018)
Copenhagen city	Hourly traffic counts registered at the permanent stations for the year 2014	Copenhagen data (2018)
Oslo city	Hourly traffic counts registered at the permanent stations for the years 2008, 2010 and 2012	Courtesy from Norwegian Road Administration
London city	Hourly traffic counts registered at the station in Marylebone Road for the years 2013 to 2016	Courtesy from Transport for London
Berlin city	Monthly and hourly profiles derived from 2014 traffic counts in the main road network	VLB (2018)
Greater Athens	Monthly, weekly and hourly profiles derived from 2006-2010 traffic counts in the main road network	Fameli and Assimakopoulos (2015)
New York City	Hourly traffic counts registered at portable stations for the years 2014 - 2018	New York City data (2019)
Mexico City	Hourly traffic counts registered at permanent stations for the year 2015	Courtesy from Secretary of Environment of Mexico City
City of Melbourne	Hourly traffic counts registered at portable stations for the years 2014 - 2017	Melbourne data (2019)
Beijing	Hourly profile derived from the traffic flows reported by the Intelligent Traffic System of Beijing	Cai and Xie (2011)
Guangzhou	Weekly and hourly profiles derived from the field investigations in Guangzhou urban/rural areas	Zheng et al. (2009)
UK	Average daily traffic flows by month, day and hour in the UK road network (2012-2016 average)	GovUK (2018)
Germany	Hourly traffic counts registered at the highways and federal highways stations for the year 2016	BASt (2018)
Spain	Hourly traffic counts registered at the national transport network for the year 2009	Courtesy from Spanish Ministry Transport
New South Wales (Australia)	Hourly traffic counts registered at permanent and sample stations for the years 2015 to 2017	TfNSW (2019)
California	Monthly, weekly and hourly profiles derived from weigh-in-motion traffic counts from 2010	McDonald et al. (2014)

1185

https://doi.org/10.5194/essd-2020-175
Preprint. Discussion started: 4 August 2020

Open Access Earth System Science Data Discussions

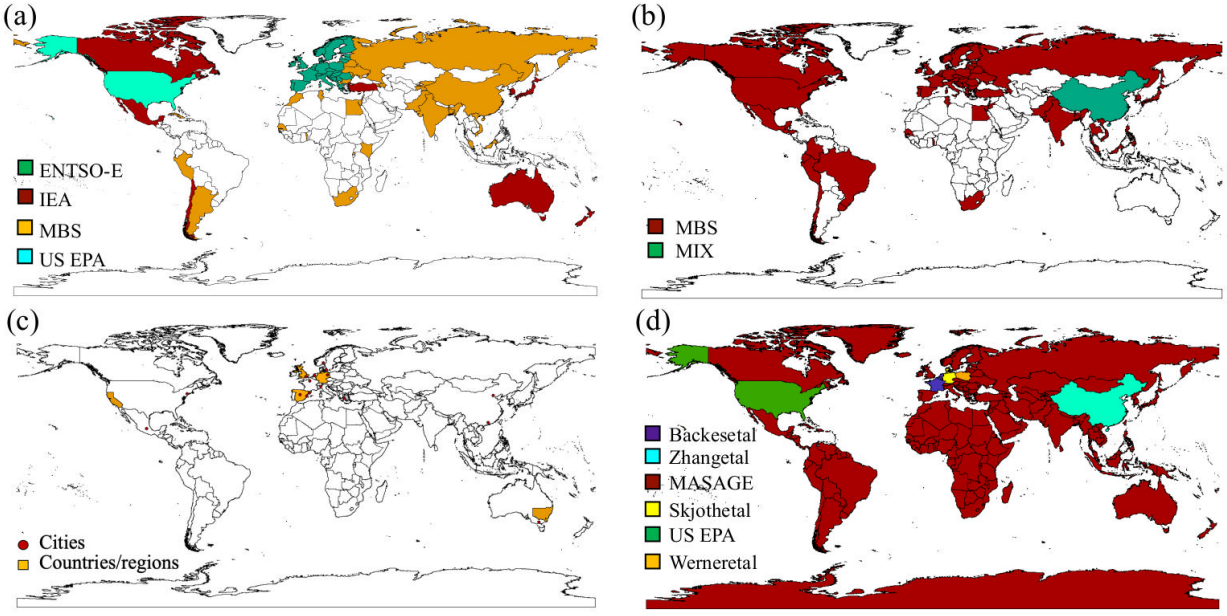

Figure 1: Representation of the spatial coverage of the datasets used to derive temporal profiles for energy industry (a), manufacturing industry (b), road transport (c) and agriculture (use of fertilizers) (d). For energy industry, the legend indicates the different sources of information used: The European Network of Transmission System Operators for Electricity (ENTSO-E), the United States Environmental Protection Agency (US EPA), The International Energy Agency (IEA) and the Monthly Bulletin of Statistics (MBS). For manufacturing industry, the legend indicates the sources of information used: the MBS and the MIX inventory (Li et al., 2017). For agriculture, sources of information are also highlighted: Backes et al. (2016), Zhang et al., (2018), the MASAGE inventory (Paulot et al., 2014), US EPA (2019), Skjoth et al. (2011), and Werner et al. (2015). Administrative boundaries are derived from GADM (2020).

https://doi.org/10.5194/essd-2020-175
Preprint. Discussion started: 4 August 2020

Open Access Earth System Science Data Discussions

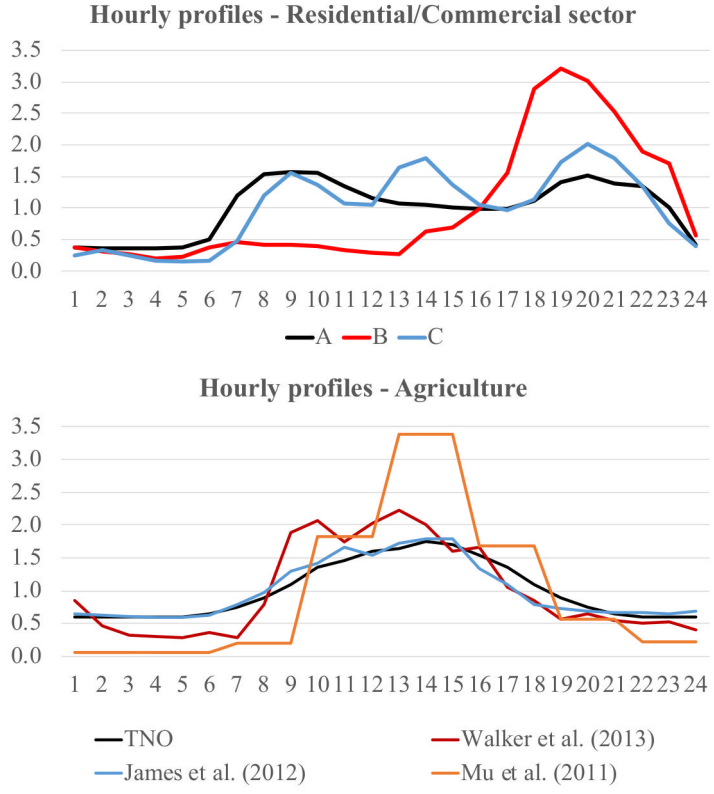

Figure 2: (Top panel) Proposed hourly temporal profiles for the residential/commercial combustion sector where profile A refers to NO_x, SO_x and CH_4 emissions in urban/rural areas of developed and developing countries, profile B refers to PM_{10}, $PM_{2.5}$, CO, CO_2, NMVOC and NH_3 in urban/rural areas of developed countries, and profile C refers to all pollutants in rural areas of developing countries. (Bottom panel) Comparison between the hourly temporal profile proposed by TNO for agricultural emissions (Denier van der Gon et al., 2011) and the three measurement-based temporal profiles reported by Walker et al. (2013) derived from NH_3 flux measurements performed in a fertilized corn canopy in North Carolina, James et al. (2012) based on direct NH_3 measurements performed in a mechanically ventilated swine barn, and Mu et al. (2011) derived from active fire satellite observations.

https://doi.org/10.5194/essd-2020-175
Preprint. Discussion started: 4 August 2020

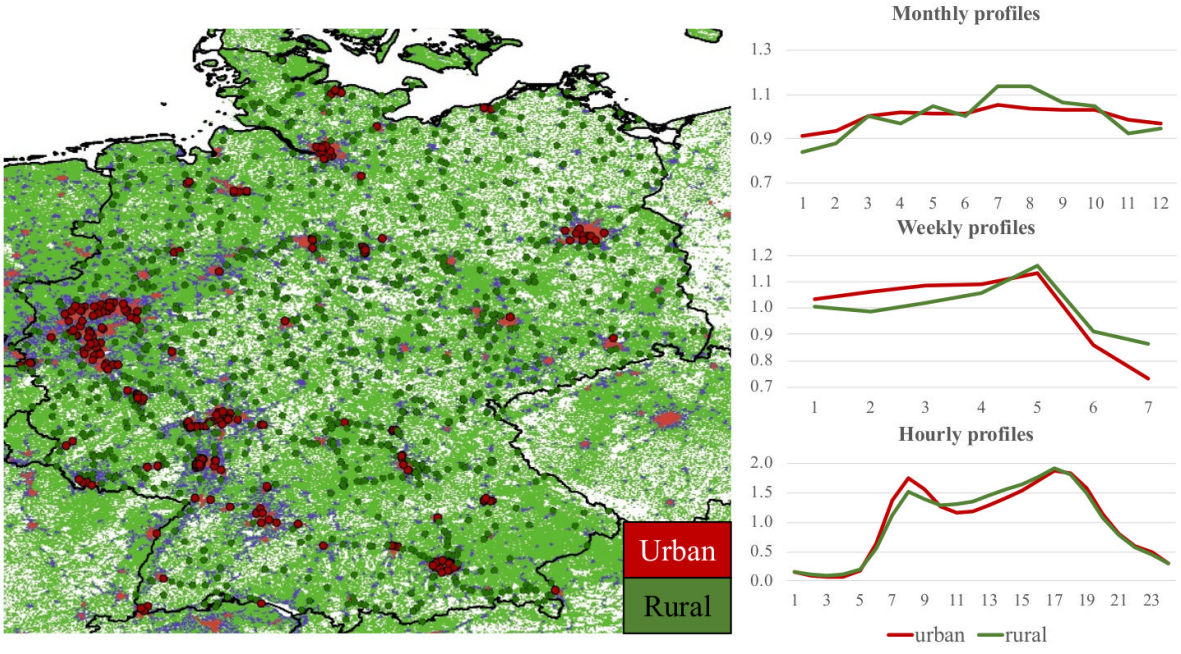

Figure 3: Map representing urban and rural human settlements in Germany as reported by the Global Human Settlement Layer (GHSL; Pesaresi et al., 2019) and the location of urban and rural German traffic count stations (left) and monthly, weekly and hourly temporal profiles derived from averaging the original traffic counts (BASt, 2018) by type of station (right). Administrative boundaries are derived from GADM (2020).

https://doi.org/10.5194/essd-2020-175
Preprint. Discussion started: 4 August 2020

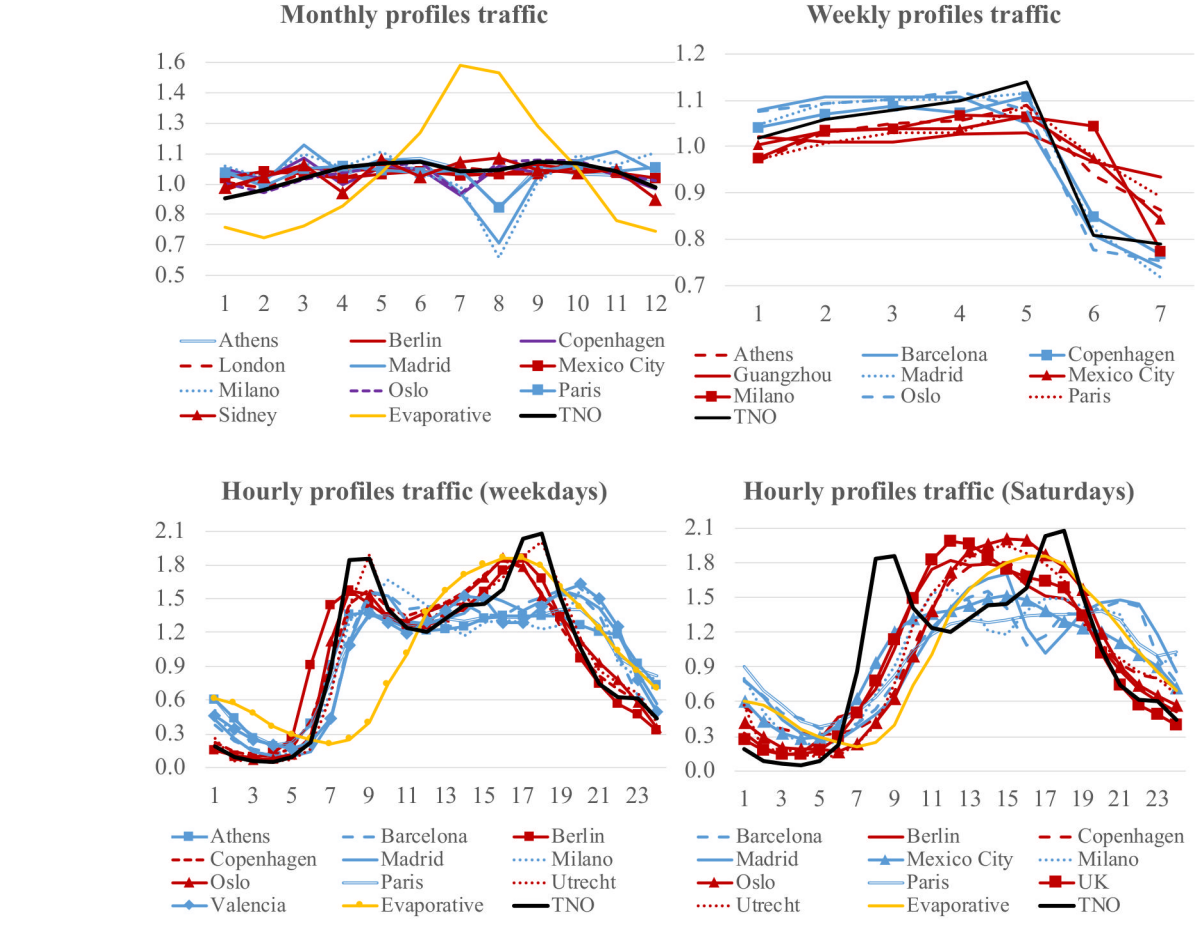

Figure 4: Monthly, weekly and hourly (for weekdays and Saturdays) temporal profiles derived from measured traffic counts in selected cities (see Table 5 for references). The profile reported by the TNO dataset is plotted for comparison purposes (Denier van der Gon et al., 2011). The monthly and hourly profiles proposed for the gasoline evaporative emissions (Evaporative, yellow line) is also shown.

https://doi.org/10.5194/essd-2020-175
Preprint. Discussion started: 4 August 2020

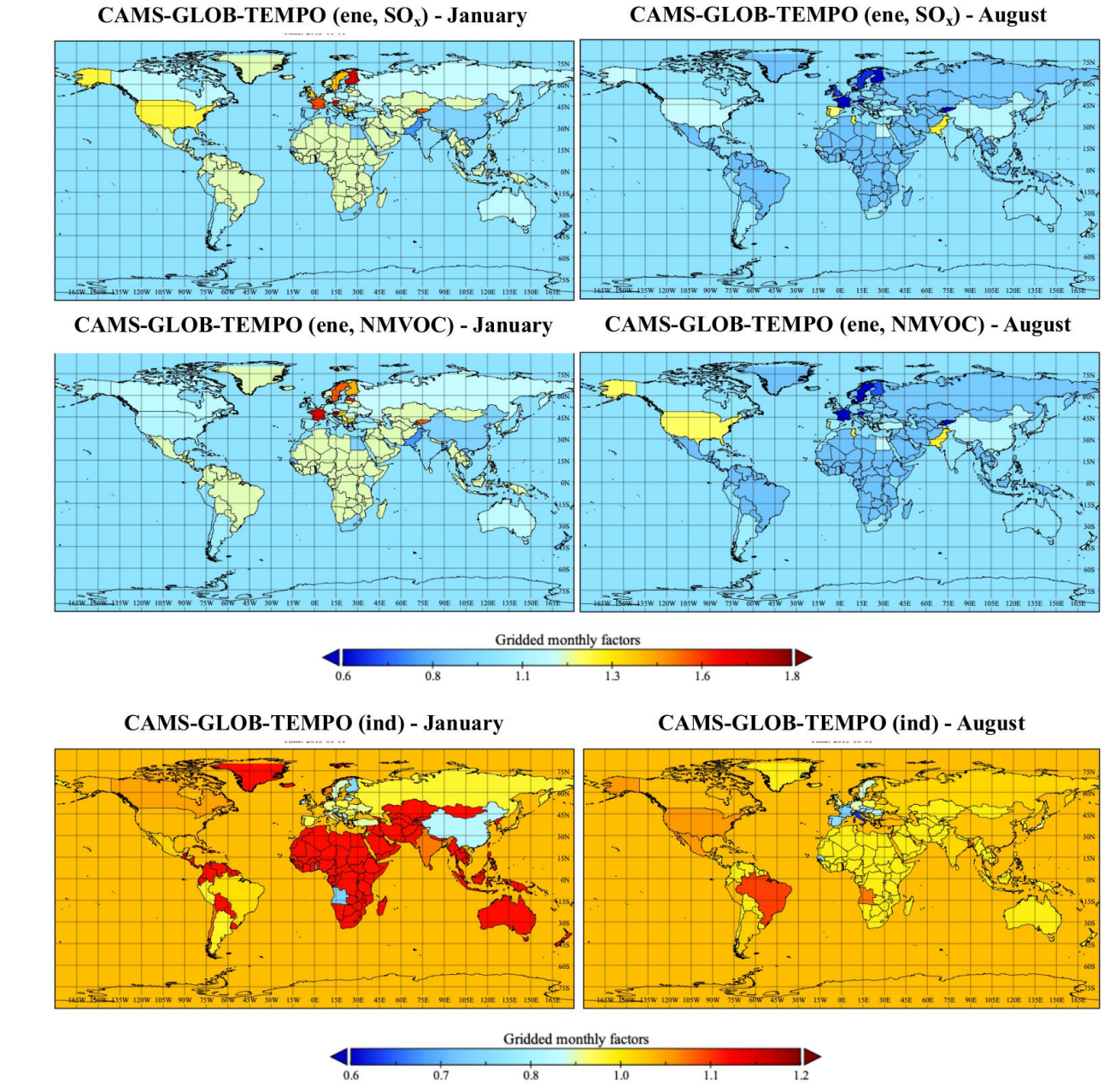

Figure 5: CAMS-GLOB-TEMPO (0.1x0.1 deg) monthly scale factor maps for NMVOC and SO_x energy industry (ene) emissions and for manufacturing industry (ind) emissions for the months of January and August. Administrative boundaries are derived from the Micro World Data Bank (MWDB2, 2011).

https://doi.org/10.5194/essd-2020-175
Preprint. Discussion started: 4 August 2020

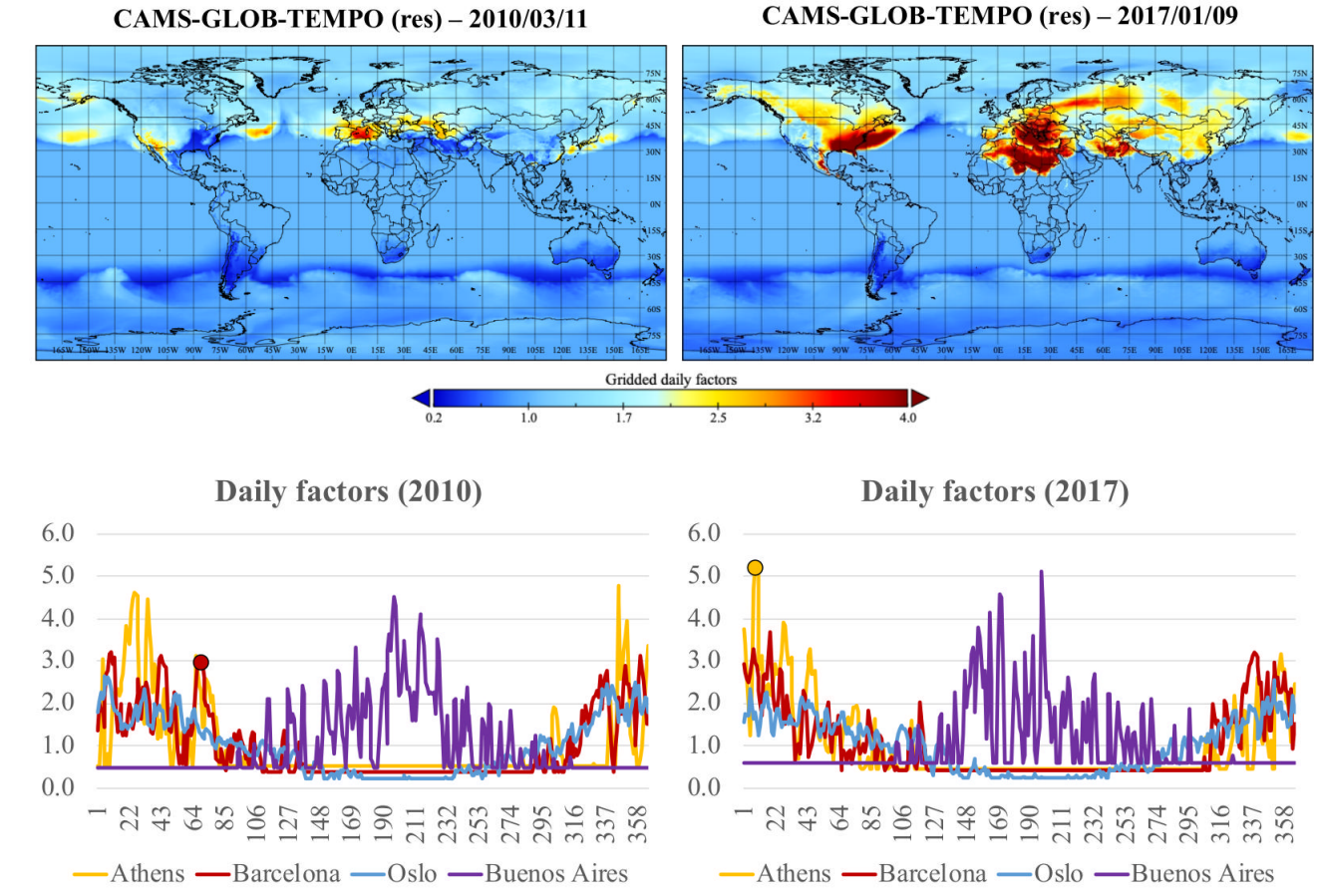

Figure 6 CAMS-GLOB-TEMPO (0.1x0.1 deg) daily scale factor maps for residential/commercial (res) emissions for 2010/03/11 and 2017/01/09. Temporal plots on the bottom represent the daily factors obtained over the cities of Athens, Barcelona, Buenos Aires and Oslo for 2010 and 2017, respectively. The red and yellow circles on the plots indicate the cold outbreaks experienced in Barcelona (2010/03/11) and Athens (2017/01/09), respectively. Administrative boundaries are derived from the Micro World Data Bank (MWDB2, 2011).

https://doi.org/10.5194/essd-2020-175
Preprint. Discussion started: 4 August 2020

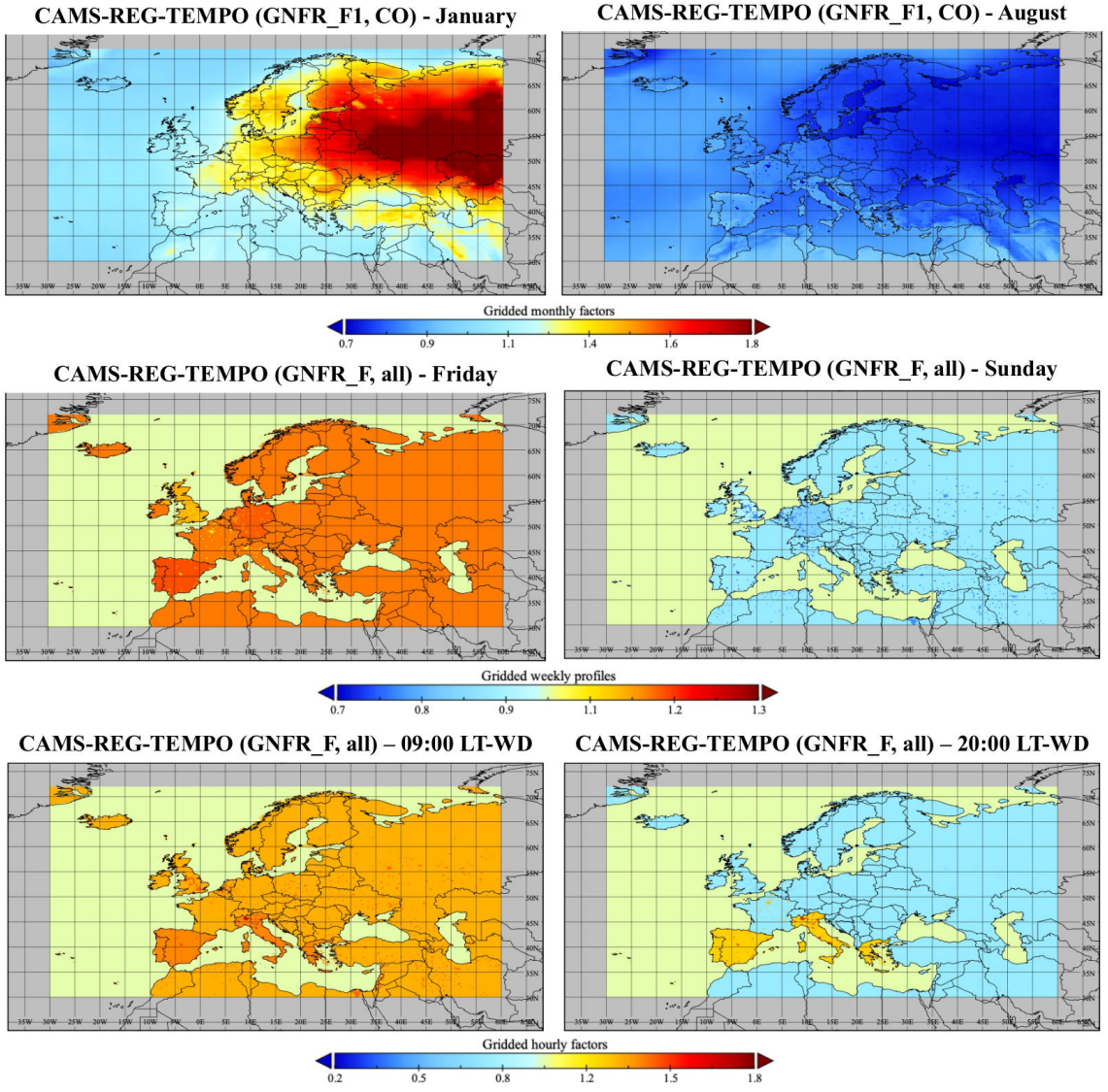

Figure 7: CAMS-REG-TEMPO (0.1x0.05 deg) monthly, weekly and hourly scale factor maps. Monthly factors correspond to the meteorological dependent profiles computed for CO exhaust gasoline emissions (GNFR_F1) for January and August (climatology of 2010-2017). Weekly factors are represented for Friday and Sunday. Hourly factors are represented for weekdays (WD) at 09:00 and 20:00 local time (LT). Administrative boundaries are derived from the Micro World Data Bank (MWDB2, 2011).

https://doi.org/10.5194/essd-2020-175
Preprint. Discussion started: 4 August 2020

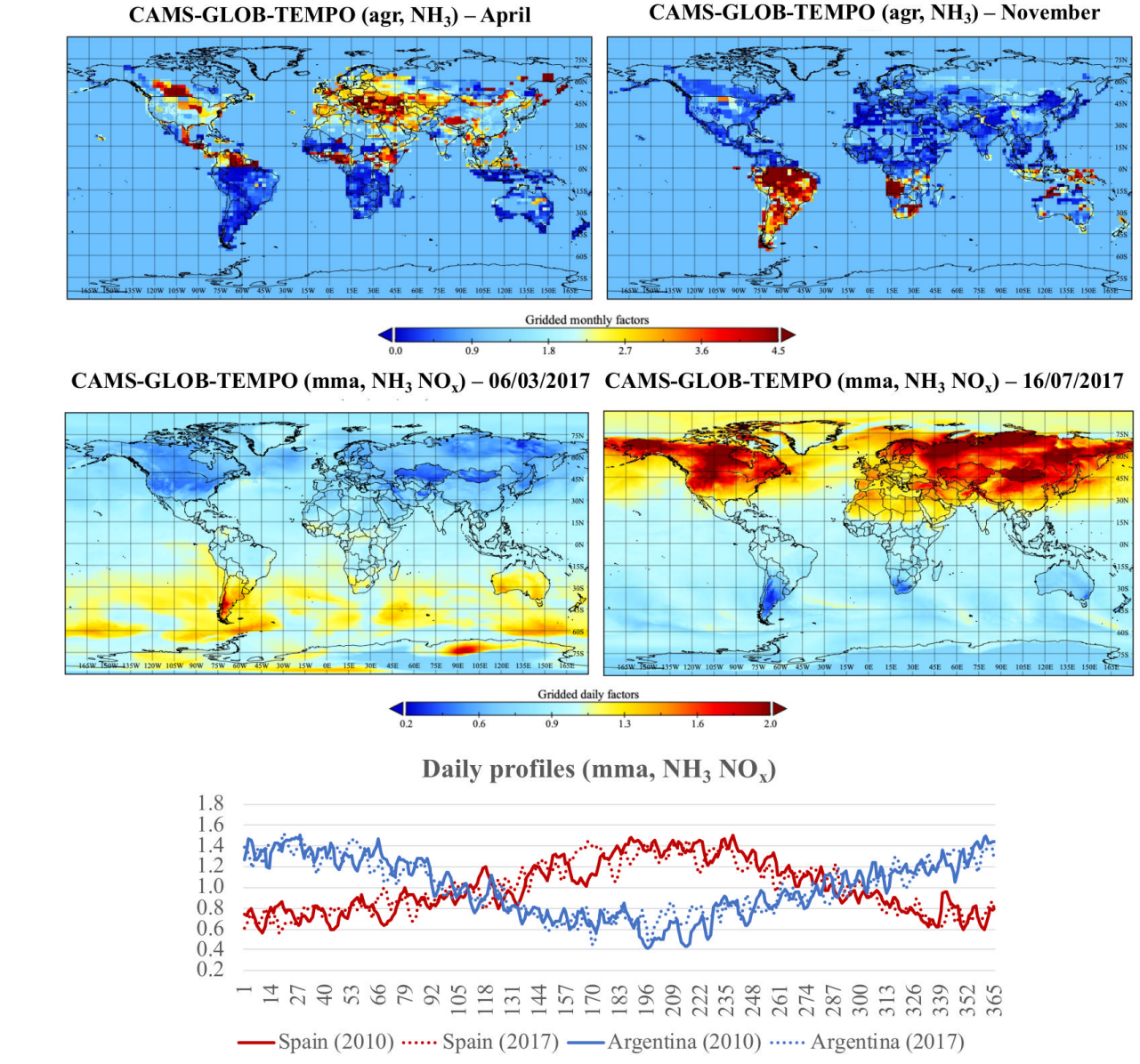

Figure 8: CAMS-GLOB-TEMPO (0.1x0.1 deg) monthly and daily scale factor maps for agriculture (agr) NH3 emissions and livestock (mma) NH3 and NOx emissions for April and November and 2017/03/06 and 2017/07/16, respectively. Temporal plots on the bottom represent the daily factors for livestock emissions (mma) obtained over Spain and Argentina for 2010 and 2017, respectively. Administrative boundaries are derived from the Micro World Data Bank (MWDB2, 2011).

https://doi.org/10.5194/essd-2020-175
Preprint. Discussion started: 4 August 2020

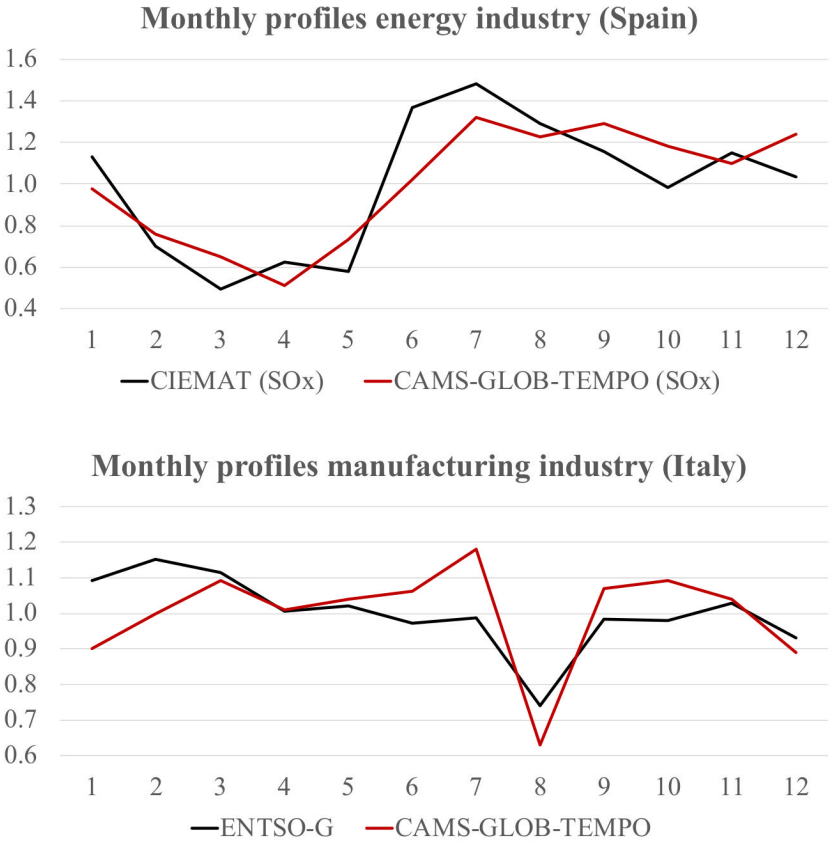

Figure 9: (Top panel) Comparison between monthly temporal factors for SO_x energy industry emissions derived from power plant emission measurements (CIEMAT, personal communication) and reported by CAMS-GLOB-TEMPO for Spain. (Bottom panel) Comparison between monthly temporal factors for manufacturing industry emissions derived from real-world measurements of industrial natural gas consumption (ENTSOG, 2020) and reported by CAMS-GLOB-TEMPO for Italy.

https://doi.org/10.5194/essd-2020-175
Preprint. Discussion started: 4 August 2020

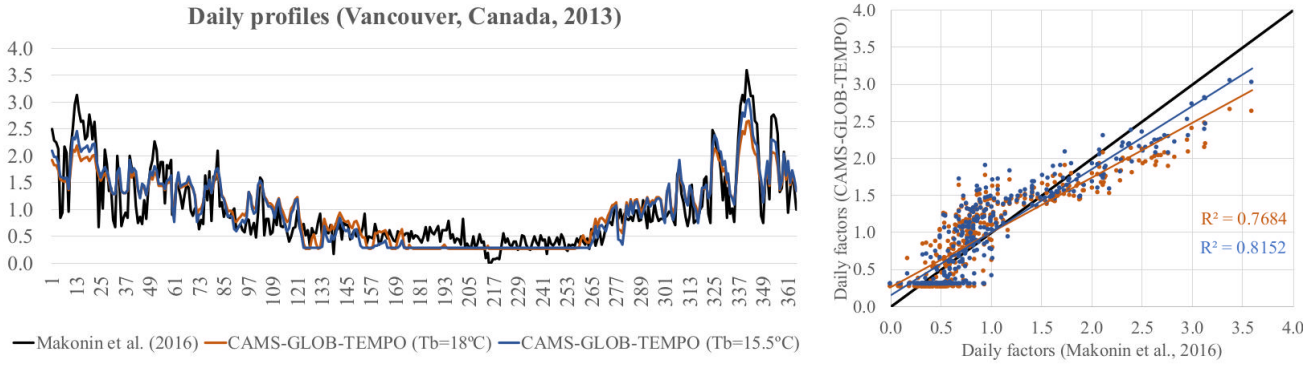

Figure 10: Comparison between daily temporal factors obtained in a location in Vancouver (Canada) for 2013 from real-world measurements of residential natural gas consumption (Makonin et al., 2016) and from the residential/commercial gridded temporal profiles reported by CAMS-GLOB-TEMPO. Two versions of the CAMS-GLOB-TEMPO temporal factors are shown as a function of the base temperature (T_b) assumed when applying the Heating Degree Day approach (18 ºC in orange and 15.5ºC in blue). The scatter plot on the bottom shows the trend lines and R^2 values obtained from the comparison between measurement-based and CAMS-GLOB-TEMPO daily factors.

https://doi.org/10.5194/essd-2020-175
Preprint. Discussion started: 4 August 2020

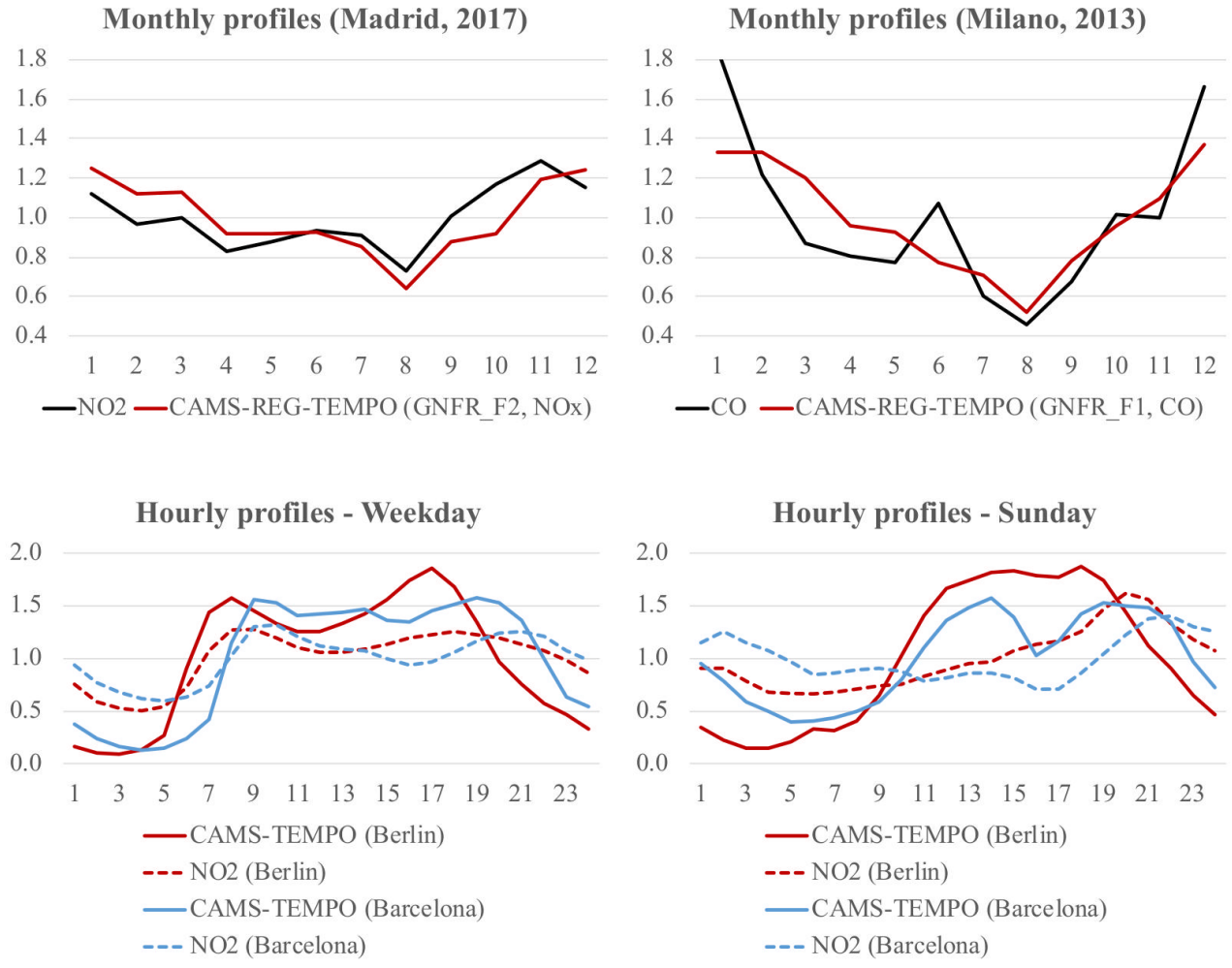

Figure 11: Comparison between monthly variations of CAMS-REG-TEMPO profiles for NO_x diesel exhaust emissions (GNFR_F2) and measured NO_2 concentrations for the city of Madrid during 2017 (top-left). Comparison between monthly variations of CAMS-REG-TEMPO profile for CO gasoline exhaust emissions (GNFR_F1) and measured CO concentrations for the city of Milano during 2013 (top-right). Hourly variation of CAMS-TEMPO GNFR_F profiles and NO_2 concentrations during weekdays (bottom-left) and Sundays (bottom-right) for the cities of Barcelona and Berlin.

https://doi.org/10.5194/essd-2020-175
Preprint. Discussion started: 4 August 2020

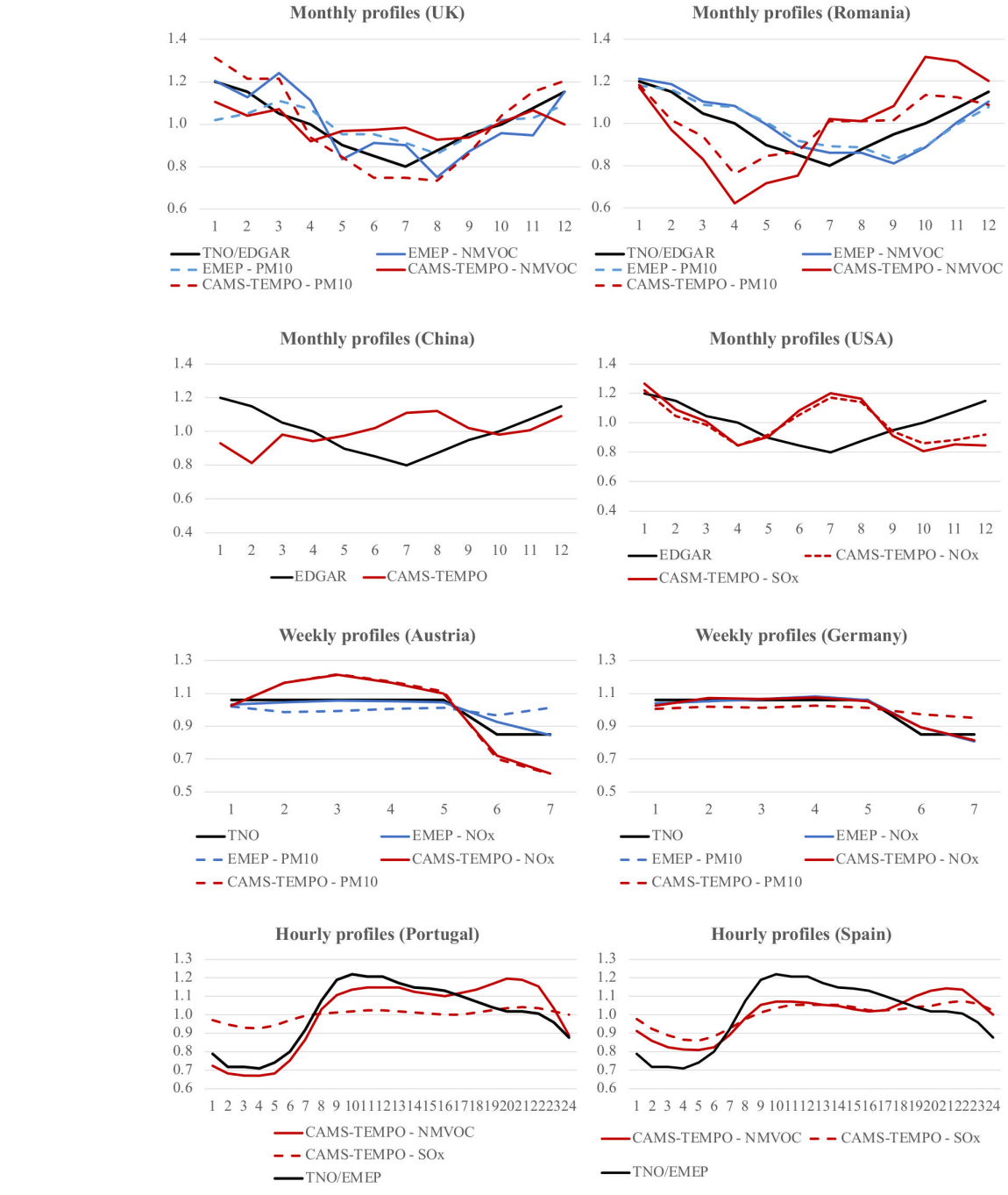

Figure 12: Comparison of monthly, weekly and hourly profiles for energy industry emissions developed in the present work (CAMS-TEMPO) with profiles from EDGAR, EMEP and TNO for selected countries.

https://doi.org/10.5194/essd-2020-175
Preprint. Discussion started: 4 August 2020

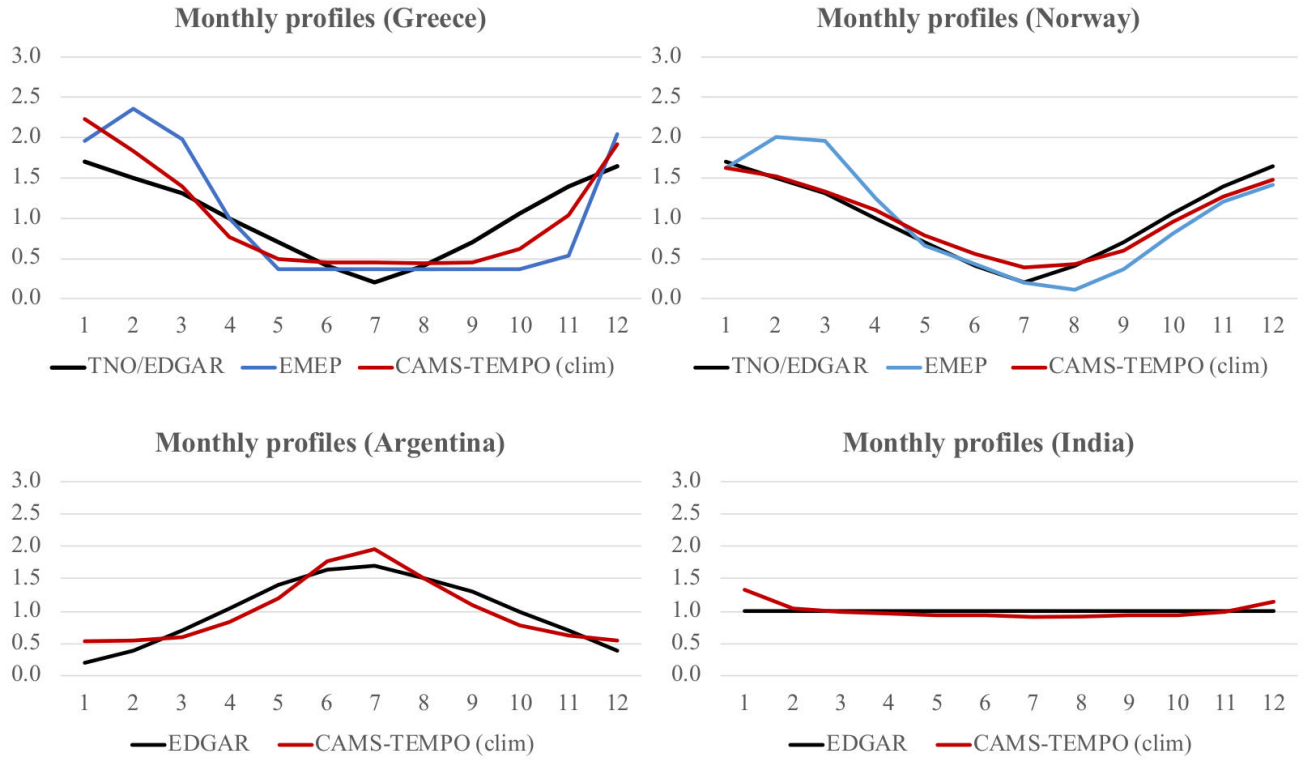

Figure 13: Comparison of monthly profiles for residential/commercial combustion emissions developed in the present work (CAMS-TEMPO) with profiles from EDGAR, EMEP and TNO for selected countries. The CAMS-TEMPO profiles represent the climatological weight factors (clim) based on the average of each month over all the available years (2010-2017).

https://doi.org/10.5194/essd-2020-175
Preprint. Discussion started: 4 August 2020

Open Access Earth System Science Data Discussions

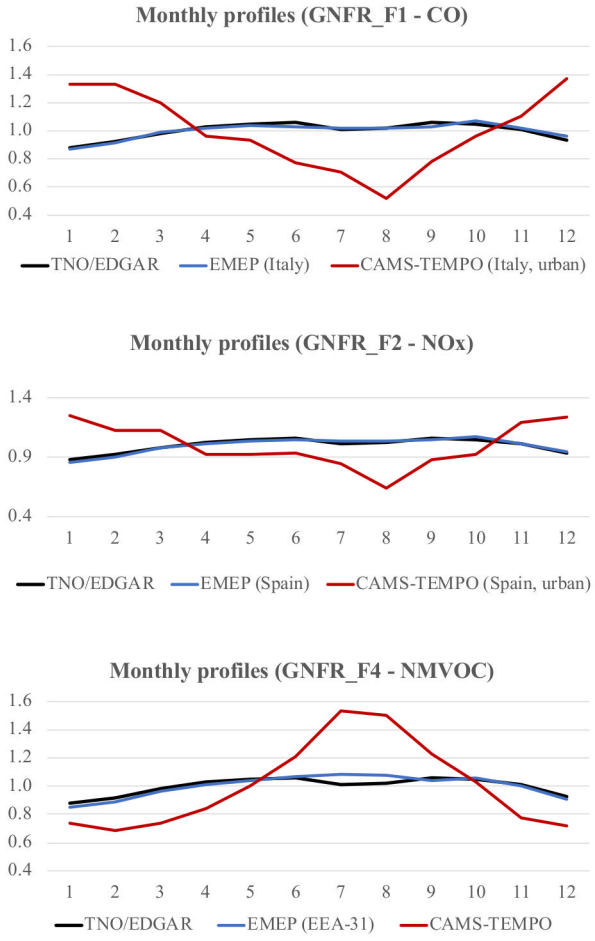

1275

Figure 14 Comparison of monthly profiles for road transport emissions developed in the present work (CAMS-TEMPO) with profiles from EDGAR, EMEP and TNO for selected countries and categories (gasoline exhaust: GNFR_F1, diesel exhaust: GNFR_F2 and non-exhaust_ GNFR_F4).

https://doi.org/10.5194/essd-2020-175
Preprint. Discussion started: 4 August 2020

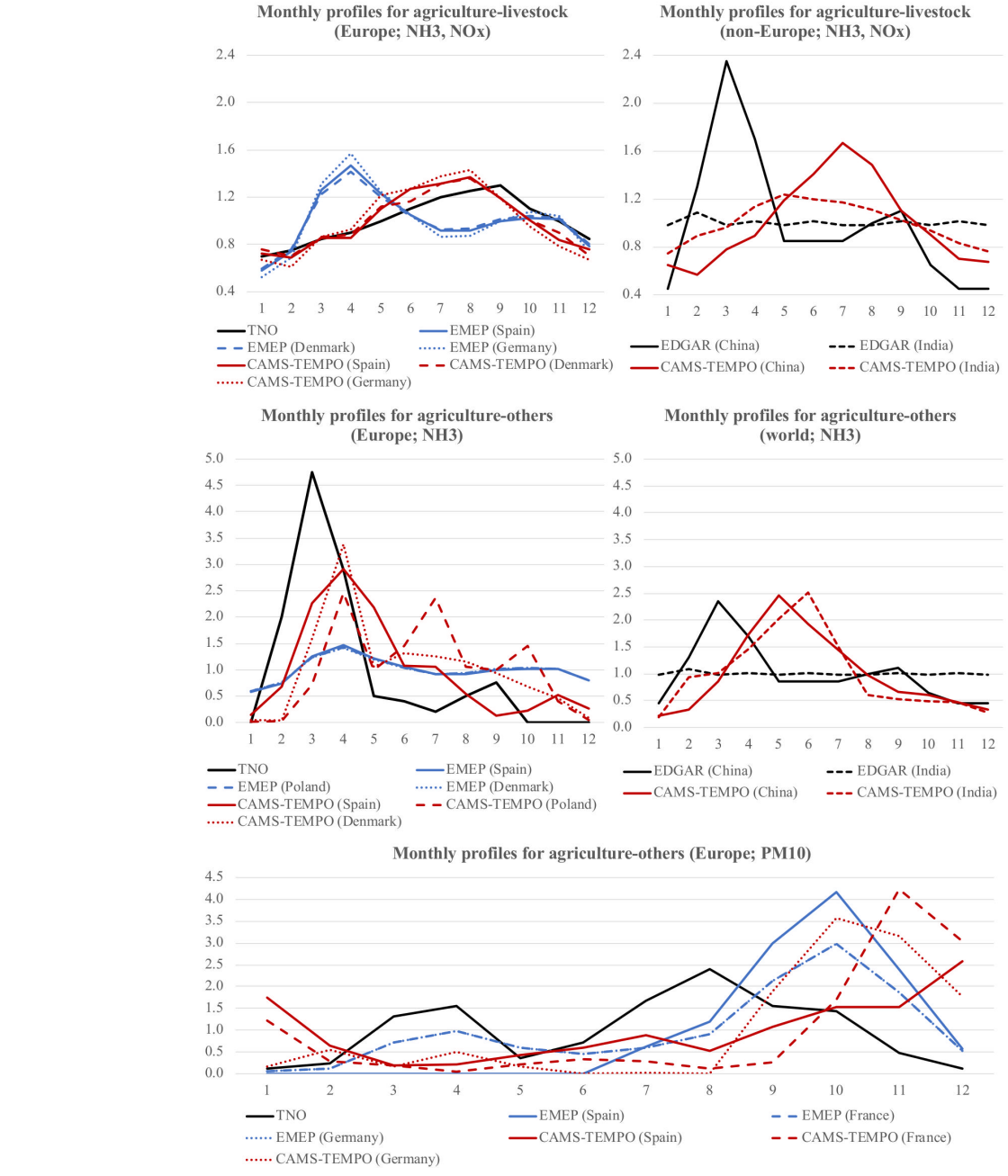

Figure 15: Comparison of monthly profiles for agricultural emissions developed in the present work (CAMS-TEMPO) with profiles from EDGAR, EMEP and TNO for selected countries.